

# OSCAR: On-Site Composition and Aesthetics Feedback through Exemplars for Photographers

Lei Yao · Poonam Suryanarayan · Mu Qiao · James Z. Wang · Jia Li

Received: date / Accepted: date

**Abstract** In this paper we describe a comprehensive system to enhance the aesthetic quality of the photographs captured by the mobile consumers. The system, named OSCAR, has been designed to provide on-site composition and aesthetics feedback through retrieved examples. We introduce three novel interactive feedback components. The first is the composition feedback which is qualitative in nature and responds by retrieving highly aesthetic exemplar images from the corpus which are similar in content and composition to the snapshot. The second is the color combination feedback which provides confidence on the snapshot to contain good color combinations. The third component is the overall aesthetics feedback which predicts the aesthetic ratings for both color and monochromatic images. An existing algorithm is used to provide ratings for color images, while new features and a new model are developed to treat monochromatic images. This system was designed keeping the next generation photography needs in mind and is the first of its kind. The feedback rendered is guiding and intuitive in nature. It is com-

puted in situ while requiring minimal input from the user.

**Keywords** Mobile · Photo Composition · Aesthetics Rating · Color Analysis · Digital Photography

## 1 Introduction

Interest in the research community on the plausibility of predicting the aesthetic quality of images has increased dramatically over the past few years. It was established in Datta et al. (2006) that photo aesthetics though being subjective can be estimated using a set of images with a general consensus on their aesthetic quality. Mathematical models could be learnt which can predict the aesthetics of any image.

Understanding aesthetics can aid many of the applications like summarization of photo collections (Obrador et al. 2010), selection of high quality images for display (Fogarty et al. 2001) and extraction of aesthetically pleasing images for image retrieval (Obrador et al. 2009). It can also be used to render feedback to the photographer on the aesthetics of his/her photographs. Many other applications have been built around suggesting improvisations to the image composition (Bhattacharya et al. 2010; Liu et al. 2001) through image re-targeting, and color harmony (Cohen-Or et al. 2006) to enhance image aesthetics. These applications are more off-line in nature. Although they are able to provide useful feedback, it is not on the spot, and requires considerable input from the user. There is no scope for any improvement on the images captured once the user moves away from the location which a professional feedback on-site can accomplish.

In order to make image aesthetic quality assessment more dynamic and to reach out for the general pub-

---

Lei Yao, Poonam Suryanarayan  
College of Information Sciences and Technology,  
The Pennsylvania State University, University Park, PA  
E-mail: luy112@ist.psu.edu

Mu Qiao  
Department of Computer Science and Engineering,  
The Pennsylvania State University, University Park, PA

James Z. Wang  
College of Information Sciences and Technology,  
The Pennsylvania State University, University Park, PA  
Office of International Science and Engineering,  
National Science Foundation, Arlington, VA

Jia Li  
Department of Statistics,  
Department of Computer Science and Engineering,  
The Pennsylvania State University, University Park, PA

lic with a practical perspective, we developed a system which can provide on-site feedback to the user. Aesthetics of an image is the result of a complex interplay of many factors like the lighting, the subject form, composition, color harmony, etc. We realized the importance of providing feedback on each of the aesthetic primitives separately by which the user infers what aspect of the photograph needs improvement and acts accordingly. We render feedback on the overall quality of the image through aesthetic ratings, the composition of the image through examples of similar images not just in terms of content but also in composition, and finally we suggest the possible good color triplets and a confidence measure on whether the image contains good combinations of colors.

There are three novel contributions in our composition and aesthetics feedback system. We will briefly introduce the concepts below and elaborate them in the subsequent sections.

The first contribution in this paper is the attempt to understand the image aesthetics from a very high-level composition perspective. We discovered that providing feedback on the composition style can help users to re-frame the subject leading to an aesthetically composed image. We recognized that the abstraction of composition can be done by analyzing the arrangement of the objects in the image. This led us to identify five different forms of compositions namely, textured images, diagonally, vertically, horizontally, and center composed images. These composition types are recognized by three classifiers, i.e. the “textured” vs “non-textured” classifier, the diagonal element detector, and the k-NN classifier for “horizontal”, “vertical” and “centered”. Understanding the composition layout of the query image facilitates the retrieval of images which are similar in composition and content.

The second contribution is providing feedback on the good color triplets present in the image. Earlier works on color harmony (Gill 2000; Sutton and Whelan 2004) were mainly driven by psychoanalysis, but we approached this problem in a data driven fashion. We analyze images from `photo.net` which received very high and very low ratings and learn a consensus on the color combinations which are predominantly found in top rated images and hence we are able to provide a confident color feedback on the major color combinations present in the image and their aesthetic compliance.

Thirdly, our contribution to this paper also includes the addition of a component to our pre-existing aesthetic quality inferencing system, ACQUINE (Datta and Wang 2010), which automatically provides aesthetic ratings for color images. This novel component instead

emphasizes on analyzing the aesthetics of black and white images, highly differ from their colored counterparts. We proposed several new promising features for indicating the aesthetic quality and trained a model based on the aesthetic rules customized to monochromatic images extracted from `dpchallenge.com`.

Casting all of these components together we have an integrated system, named OSCAR (On-Site Composition and Aesthetics feedback through exemplars). The system can be easily ported onto a mobile device which travels with the user or can be seen as a remote server which can be accessed through the 3G or 4G networks, bringing the research closer to the user. This system can further be customized into creating personal tutor, which is able to provide feedback based on the user’s past photo-taking behavior.

The rest of the paper is organized as follows. The system architecture is introduced in Section 1.1. We discuss the spatial composition classification in Section 2. Color combination feedback is discussed in Section 3. We then describe, in Section 4, the aesthetic feedback on both color and monochromatic images. Experimental results and user studies are presented in Section 5 and Section 6. Time analysis is reported in Section 7. Finally, we conclude and discuss future work in Section 8.

## 1.1 System Architecture

Figure 1 shows the architecture of our proposed system. Future generations of digital cameras can access the 3G or 4G network and have substantial internal computational power, the same way as today’s smart phones. Some current camera phones, e.g., the iPhone and the Nokia N73 phone, can send photos to a remote server on the Internet and receive feedback from the server.<sup>1</sup> As a photographer shoots, the photo is sent via the network to a cloud server. Our system on the server side will provide immediate aesthetic quality assessment on the visual characteristics of the submitted photos, analyze their composition and color properties, and send on-site feedback to photographers. As shown in Figure 1, the system comprises of several modules.

The **image archive** is used to store all the submitted images, which are labeled as “color images” and “monochromatic images”. Given an input image, the **composition analyzer** will analyze its composition properties from different perspectives. For example, visual elements with great compositional potential, such as diagonals and curves, will be detected. Photographs

<sup>1</sup> <http://www.wired.com/gadgetlab/2010/07/nadia-camera-offers-opinion-of-your-terrible-photos/>

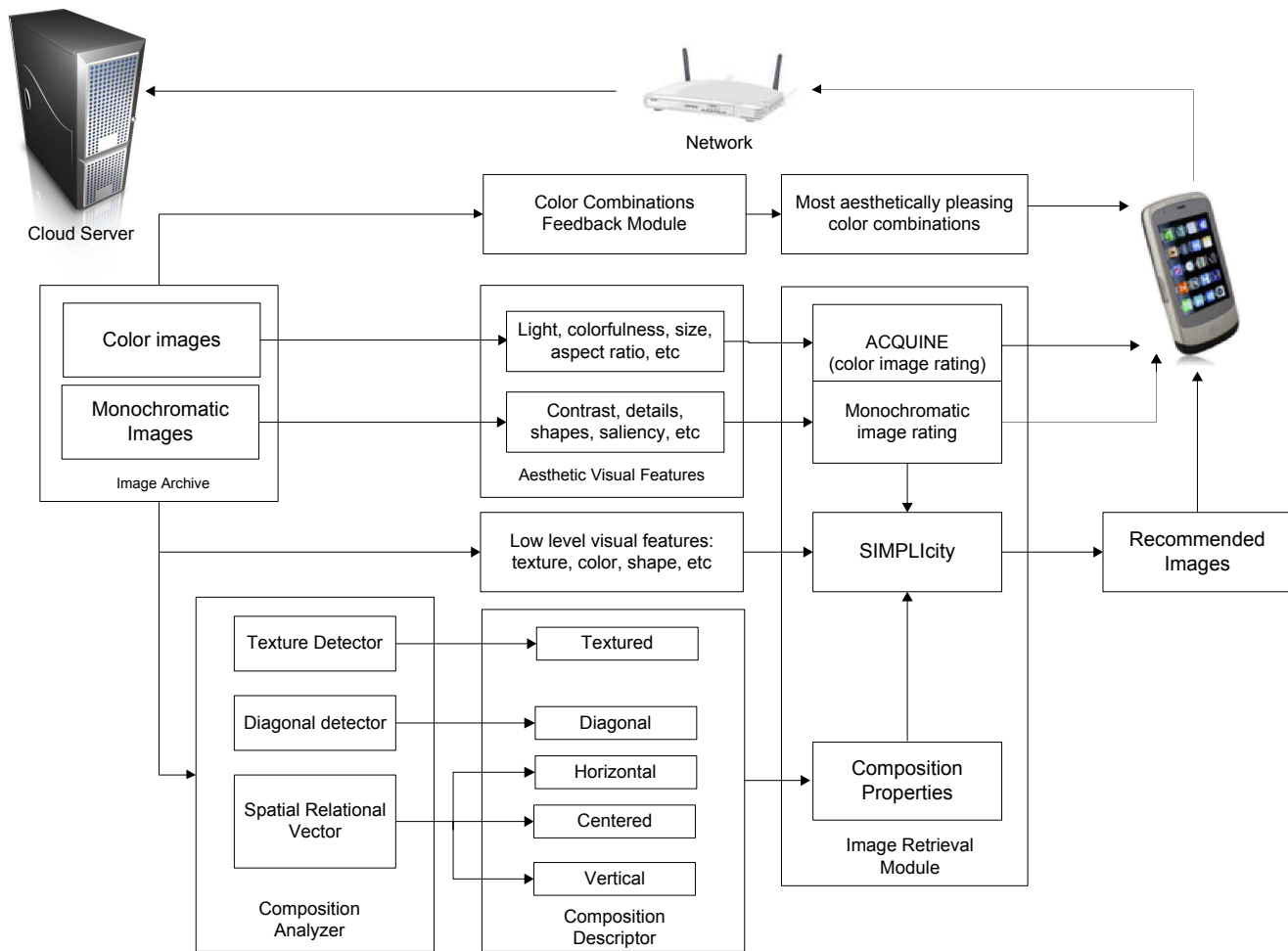


**Fig. 1** The architecture of our composition and aesthetics feedback system.

will be categorized by high-level composition properties. Specifically, the composition analyzer performs spatial composition categorization. Currently, we consider five categories, namely, “textured”, “diagonal”, “horizontal”, “centered”, and “vertical”. Composition-related qualities, e.g., visual balance and simplicity of background, can also be evaluated. Images similar in composition as well as content can be retrieved from a database of photos with high aesthetic ratings so that the photographer can learn through examples. In addition to detecting compositional characteristics, a more constructive feedback to users can be provided in the future through automatic composition correction, where the image is either cropped or tilted to attain better composition. In the current work, we have not ventured far in this direction, and our focus will be on retrieving exemplar images.

The **color combination feedback module** will find the most aesthetically pleasing color combination from that image, with a score indicating the confidence

of having high quality. At the same time, some aesthetics related visual features are extracted. For instance, we extract from color images such features as light, colorfulness, size, and aspect ratio, which are provided to ACQUINE for aesthetic quality assessment. We have also developed a similar assessment module for monochromatic images, which incorporates some other features like contrast, details, shapes, saliency, etc.

In the **retrieval module**, a ranking schema is designed to integrate the composition properties and aesthetic rating into SIMPLicity, an image retrieval system based on color, texture and shape features (Wang et al. 2001). Images with high aesthetic ratings, as well as similar composition properties and visual features, are retrieved. An effective way to learn photography is through observing master works and imitating. Practicing good compositions in the field helps develop creative sensibility and unique styling. Especially for beginners, well-composed photographs are valuable learning resources. By retrieving high quality, similarly com-

posed photographs, our system can provide users with practical assistance in improving photography composition.



**Fig. 2** User interface of OSCAR mobile application. Left: photo submitted to the server, best color triplets and its confidence score, aesthetics score of the photo (scores are indicated by bar). Right: similarly composed exemplars retrieved from the database.

## 1.2 User Interaction with the System

Figure 2 shows an interface of the mobile application under development. User interaction and the ease of usage are among the main concerns for the mobile application to be successful. Our present system requires very little user input and is minimalistic in nature. Once the user takes a snapshot he/she can choose to send the image to our cloud server for feedback on composition and aesthetics. Based on the feedback the user can go on to improve the composition of image by taking newer snaps of the subject and at the same time understand the characteristics in which the photograph might need improvement. A Web-based demonstration of the proposed system is made available at <http://acquine.alipr.com/oscar/>.

## 2 Spatial Composition Categorization

Composition is the art of putting things together with conscious thoughts. In photography, it concerns the arrangement of various visual elements, such as line, color, space, etc. Composition is closely related to the aesthetic qualities of photographs. To the best of our knowledge, very few works have been done on photography composition in image processing and computer vision.

Here we study photography composition from the perspective of spatial layout, which is about how visual elements are geometrically arranged in a picture.

After studying many guiding principles in photography, we find that there are several typical spatial layouts. Our goal is to automatically classify major types of spatial layouts. In this paper, we will consider the following typical spatial composition categories: “horizontal”, “vertical”, “centered”, “diagonal”, and “textured”.

According to long-existing photography principles, lines formed by linear elements are important because they lead the eye through the image and contribute to the mood of the photograph. Horizontal, vertical, and diagonal lines are associated with serenity, strength, and dynamism respectively (Krages 2005). We thus include “horizontal”, “vertical”, and “diagonal” as three composition categories. Photographs with a centered main subject and a clear background fall into the category “centered”. By “textured”, we mean that the whole image appears like a patch of texture or a relatively homogeneous pattern, for example, an image of a brick wall.

The five categories of composition are not mutually exclusive. We apply several classifiers sequentially to an image: “textured” versus “non-textured”, “diagonal” versus “non-diagonal”, and finally a possibly overlapping classification of “horizontal”, “vertical”, and “centered”. For example, an image can be classified as “non-textured”, “diagonal”, and “horizontal”. We use a method in Wang et al. (2001) to classify “textured” images. It has been demonstrated that retrieval performance can be improved for both textured and non-textured images by first classifying them (Wang et al. 2001). The last two classifiers are developed in the current work, with details to be presented in a short while.

A conventional image retrieval system returns images according to visual similarity. However a photographer’s intention is more likely to search for pictures by composition rather than by visual details. We therefore integrate composition classification into the SIMPLICITY image retrieval system (Wang et al. 2001) so that retrieved images will tend to have similar composition. Furthermore, we provide the option to rank retrieved images by their aesthetic ratings.

### 2.1 Dataset

The spatial composition classification method is tested on a dataset crawled from [photo.net](http://photo.net), a photography community where peers can share, rate, and critique photos. These photographs are mostly general-purpose

pictures and have a wide range of aesthetic quality. Among the crawled photos, a large proportion have frames which will distort the visual content in image processing and impact analysis results. Therefore we remove frames from the original images in a semi-automatic fashion. The images which contain frames are picked manually and a program is used to remove simple frames with flat tones. Frames embedded with pattern or text usually cannot be correctly removed, and these photos are simply removed from the dataset when we re-check the cropped images in order to make sure the program has correctly removed the frames from images. We construct a dataset with 13,302 unframed pictures. Those pictures are then rescaled so that the long dimension of the image has at most 256 pixels. We manually labeled 222 photos, among which 50 are horizontally composed, 51 are vertically composed, 50 are centered, and 71 are diagonally composed. Our classification algorithms are developed and evaluated based on the manually labeled dataset. The entire dataset will be used in system performance evaluation.

## 2.2 “Textured” vs “Non-textured” Classifier

We use the “textured” vs “non-textured” classifier in SIMPLIcity to separate textured images from the rest. The algorithm is motivated by the observation that if pixels in a textured area are clustered using local features, each cluster of pixels yielded will be scattered across the area due to the homogeneity appearance of texture. While for non-textured images, the clusters tend to be clumped. An image is divided evenly into  $4 \times 4 = 16$  large blocks. The algorithm thus calculates the proportion of pixels in each cluster that belong to any of the 16 blocks. If the cluster of pixels is scattered over the whole image, the proportions over the 16 blocks are expected to be roughly uniform. For each cluster, the  $\chi^2$  statistic is computed to measure the disparity between the proportions and the uniform distribution over the 16 blocks. The average value of the  $\chi^2$  statistics for all the clusters is then thresholded to decide whether an image is textured or not.

## 2.3 Diagonal Element Detection

Diagonal elements are strong compositional constituents. The diagonal rule in photography states that a picture will appear more dynamic if the objects fall or follow a diagonal line. Photographers often use diagonal elements as the visual path to draw viewers’ eyes through

the image.<sup>2</sup> By visual path, we mean the path of eye movement when viewing a photograph (Warren 2002). When such a visual path stands out in the picture, it also has the effect of uniting individual parts in a picture. The power of the diagonal lines for composition was exploited very early on by artists. Speed (1972) discussed in great details how Velazquez used the diagonal lines to unite a picture in his painting “The Surrender of Breda”.

Because of the importance of diagonal visual paths for composition, we create a spatial composition category for diagonally composed pictures. More specifically, there are two subcategories, diagonal from upper left to bottom right and from upper right to bottom left. We declare the composition of a photo as diagonal if diagonal visual paths exist.

Detecting the exact diagonal visual paths is difficult. Segmented regions or edges provided by the usual image processing techniques often can only serve as *ingredients*, aka, local patterns, either because of the nature of the picture or the limitation of the processing algorithms. In contrast, an *element* refers to a global pattern, e.g., a broken straight line (multiple edges) that has presence in a large area of the image plane.

We learned from tutorials and textbooks the following principles, and design accordingly our algorithm for detecting diagonal visual paths. We present some of the principles in the diagonal case, but they apply similarly to other directional visual paths.

1. **Principle of multiple visual types:** Lines are effective design elements in creating compositions, but “true” lines rarely exist in real world. Lines we perceive in photographs usually belong to one of these types: outlines of forms; narrow forms; lines of arrangement; and lines of motion or force (Feininger 1973). We do not restrict diagonal elements to actual diagonal lines of an image plane. They could be the boundary of a region, a linear object, and even an imaginary line along which different objects align. Linear objects, such as pathways, waterways, and the contour of a building, can all create visual paths in photographs. When placed diagonally, they are generally perceived as more dynamic and interesting than other compositions. Figure 3 shows examples of using diagonal compositions in photography.
2. **Principle of wholes/Gestalt Law:** Gestalt psychologists studied early on the phenomenon of human eyes perceiving visual components as organized patterns or wholes, known as the Gestalt law of or-

<sup>2</sup> <http://www.digital-photography-school.com/using-diagonal-lines-in-photography>

ganization. According to the Gestalt Law, the factors that aid in human visual perception of forms include Proximity, Similarity, Continuity, Closure, and Symmetry (Sternberg et al. 2008).

3. **Principle of tolerance:** Putting details along diagonals creates more interesting compositions. Visual elements such as lines and regions slightly off the ideal diagonal direction can still be perceived as diagonal and are usually more natural and interesting.<sup>3</sup>
4. **Principle of prominence:** A photograph can contain many lines, but dominant lines are the most important in regard to the effect of the picture (Folts 2005).<sup>4</sup> Visual elements need sufficient span along the diagonal direction in order to strike a clear impression.

Following the above principles, we first find diagonal ingredients from low-level visual cues using both regions obtained by segmentation and connected lines obtained by edge detection. Then, we apply the Gestalt Law to merge the ingredients into elements, i.e., more global patterns. The prominence of each merged entity is then assessed. Next, we describe the algorithms for detecting diagonal visual paths using segmented regions and edges respectively.

### 2.3.1 Diagonal Segment Detection

Image segmentation is often used to simplify the image representation. It can generate semantically meaningful regions that are easier for analysis. This section describes our approach to detecting diagonal visual paths based on segmented regions. We use the recently developed image segmentation algorithm (Li 2011) for it achieves state-of-the-art accuracy at a speed sufficiently fast for real-time systems. The algorithm also ensures that the segmented regions are spatially connected, a desirable trait many algorithms do not possess.

After image segmentation, we find the orientation of each segment, defined as the orientation of the moment axis of the segment. The moment axis is the direction along which the spatial locations of the pixels in the segment have maximum variation. It is the first principal component direction for the data set containing the coordinates of the pixels. For instance, if the segment is an ellipse (possibly tilted), the moment axis is simply the long axis of the ellipse. The orientation of the moment axis of a segmented region measured in degrees is computed according to Russ (2006).

<sup>3</sup> <http://www.picture-thoughts.com/photography/composition/angle/>

<sup>4</sup> <http://www.great-landscape-photography.com/photography-composition.html>

Next, we apply the Gestalt Law to merge certain segmented regions in order to form visual elements. Currently, we only deal with a simple case of disconnected visual path, where the orientations of all the disconnected segments are diagonal.

Let us introduce a few notations before describing the rules for merging. We denote the normalized column vector of the diagonal direction by  $\mathbf{v}_d$  and that of its orthogonal direction by  $\mathbf{v}_d^c$ . We denote a segmented region by  $S$ , which is a set of pixel coordinates  $\mathbf{x} = (x_h, x_v)^t$ . The projection of a pixel with coordinate  $\mathbf{x}$  onto any direction characterized by its normalized vector  $\mathbf{v}$  is the inner product  $\mathbf{x} \cdot \mathbf{v}$ . The projection of  $S$  onto  $\mathbf{v}$ , denoted by  $\mathcal{P}(S, \mathbf{v})$ , is a set containing the projected coordinates of all the pixels in  $S$ . That is,  $\mathcal{P}(S, \mathbf{v}) = \{\mathbf{x} \cdot \mathbf{v} : \mathbf{x} \in S\}$ . The length (also called spread) of the projection  $|\mathcal{P}(S, \mathbf{v})| = \max_{\mathbf{x}_i, \mathbf{x}_j \in S} |\mathbf{x}_i \cdot \mathbf{v} - \mathbf{x}_j \cdot \mathbf{v}|$  is the range of values in the projected set.

The rules for merging, called ‘‘Similarity’’, ‘‘Proximity’’, and ‘‘Continuity’’, are listed below. Two segments satisfying all of the rules are merged.

- **Similarity:** Two segments  $S_i$ ,  $i = 1, 2$ , with orientations  $e_i$ ,  $i = 1, 2$ , are similar if the following criteria are satisfied:

1. Let  $[\tilde{\varphi}, \hat{\varphi}]$  be the range for nearly diagonal orientations.  $\tilde{\varphi} \leq e_i \leq \hat{\varphi}$ ,  $i = 1, 2$ . That is, both  $S_1$  and  $S_2$  are nearly diagonal.
2. The orientations of  $S_i$ ,  $i = 1, 2$ , are close:

$$|e_1 - e_2| \leq \beta, \text{ where } \beta \text{ is a pre-chosen threshold.}$$

3. The lengths of  $\mathcal{P}(S_i, \mathbf{v}_d)$ ,  $i = 1, 2$ , are close:

$$r = \frac{|\mathcal{P}(S_1, \mathbf{v}_d)|}{|\mathcal{P}(S_2, \mathbf{v}_d)|}, \quad r_1 \leq r \leq r_2,$$

where  $r_1 < 1$  and  $r_2 > 1$  are pre-chosen thresholds.

- **Proximity:** Segments  $S_i$ ,  $i = 1, 2$ , are proximate if their projections on the diagonal direction,  $\mathcal{P}(S_i, \mathbf{v}_d)$ ,  $i = 1, 2$ , are separated by less than  $p$ , and the overlap of their projections is less than  $q$ .
- **Continuity:** Segments  $S_i$ ,  $i = 1, 2$ , are continuous if their projections on the direction orthogonal to the diagonal,  $\mathcal{P}(S_i, \mathbf{v}_d^c)$ ,  $i = 1, 2$ , are overlapped.

We now describe how we choose the various thresholds.

1.  $\beta = 10^\circ$ .
2.  $r_1 = 0.8$ ,  $r_2 = 1.25$ .
3. The values of  $p$  and  $q$  are decided adaptively according to the sizes of  $S_i$ ,  $i = 1, 2$ . Let the spread of  $S_i$  along the diagonal line be  $\lambda_i = |\mathcal{P}(S_i, \mathbf{v}_d)|$ . Then  $p = k_p \min(\lambda_1, \lambda_2)$  and  $q = k_q \min(\lambda_1, \lambda_2)$ , where  $k_p = 0.5$  and  $k_q = 0.8$ .

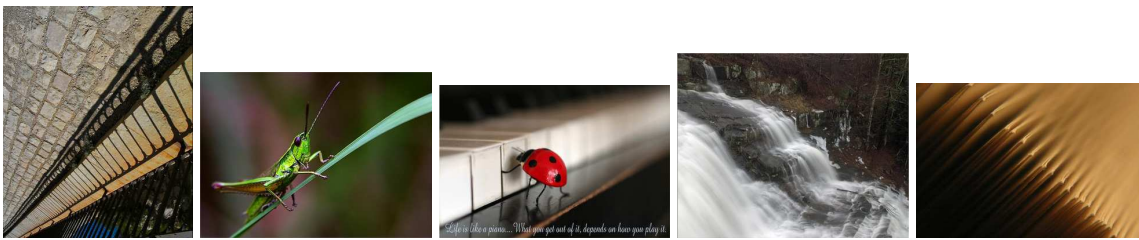


Fig. 3 Photographs of diagonal composition.

The value of  $p$  determines the maximum gap allowed between two disconnected segments to continue a visual path. The wider the segments spread over the diagonal line, the more continuity they present to the viewer. Therefore, heuristically, a larger gap is allowed, which is why  $p$  increases with the spreads of the segments. On the other hand,  $q$  determines the extent of overlap allowed for the two projections. By a similar rationale,  $q$  also increases with the spreads. If the projections of the two segments overlap too much, the segments are not merged because the combined spread of the two differs little from the individual spreads.

4. The angular range  $[\tilde{\varphi}, \hat{\varphi}]$  for nearly diagonal orientations is determined adaptively according to the geometry of the rectangle bounding the image.

As stated in Lamb et al. (2010), one practical extension of the diagonal rule is to have the objects fall within two boundary lines parallel to the diagonal. These boundary lines are one-third of the perpendicular distance from the diagonal to the opposite vertex of the rectangular photograph. This diagonal stripe area is shown in Figure 4(b). A similar suggestion is made in an online article,<sup>3</sup> where boundary lines are drawn using the so-called sixth points on the borders of the image plane. A sixth point along the horizontal border from the upper left corner locates on the upper border and is away from the corner by one-sixth of the image width. Similarly, we can find other sixth (or third) points from any corner and either horizontally or vertically.

Suppose we look for an approximate range for the diagonal direction going from the upper left corner to the bottom right. The sixth and third points with respect to the two corners are found. As shown in Figure 4(a), these special points are used to create two stripes marked by lime and blue colors respectively. Let the orientations of the lime stripe and the blue stripe in Figure 4(a) be  $\varphi_1$  and  $\varphi_2$ . Then we set  $\tilde{\varphi} = \min(\varphi_1, \varphi_2)$ , and  $\hat{\varphi} = \max(\varphi_1, \varphi_2)$ . A direction  $\mathbf{v} \in [\tilde{\varphi}, \hat{\varphi}]$  is claimed nearly diagonal. Similarly, we can obtain the angular range for the diagonal direction from the upper right corner to the bottom left. The reason to use the orientations of the stripes instead of nearly diagonal bounding

lines is that when the width and the height of an image are not equal, the orientation of a stripe will twist toward the elongated side to some extent.

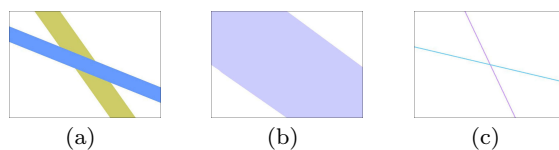


Fig. 4 Diagonal orientation bounding conditions.

From now on, a segment can be a merged entity of several segments originally given by the segmentation algorithm. For brevity, we still call the merged entity a segment. Applying the principle of tolerance, we filter out a segment from diagonal if its orientation is outside the range  $[\tilde{\varphi}, \hat{\varphi}]$ , the same rule applied to the smaller segments before merging.

After removing non-diagonal segments, at last, we apply the principle of prominence to retain only segments with a significant spread along the diagonal direction. For segment  $S$ , if  $|\mathcal{P}(S, \mathbf{v}_d)| \geq k_l \times l$ , where  $l$  is the length of the diagonal line and  $k_l = \frac{2}{3}$  is a threshold, the segment is declared a diagonal visual path. It is observed that a diagonal visual path is often a merged entity of several small segments originally produced by the segmentation algorithm, which are not prominent individually.

### 2.3.2 Diagonal Edge Detection

According to the principle of multiple visual types, besides segmented regions, lines and edges can also form visual paths. Moreover, segmentation can be unreliable sometimes because over-segmentation and under-segmentation often cause diagonal elements to be missed. We observe that among photographs showing diagonal composition, many contain linear diagonal elements. Those linear diagonal elements usually have salient boundary lines along the diagonal direction, which can be found through edge detection. Therefore we use edges as another visual cue, and combine the results obtained

based on both edges and segments to increase the sensitivity of detecting diagonal visual path.

We use the Edison edge detection algorithm (Meer and Georgescu 2001). It has been experimentally demonstrated that Edison edge detection can generate cleaner edge maps than many other methods (Meer and Georgescu 2001). We examine all the edges to find those oriented diagonally and significant enough to be a visual path.

Based on the same set of principles, the whole process of finding diagonal visual paths based on edges is similar to the detection of diagonal segments. The major steps are described below. We denote an edge by  $E$ , which is a set of coordinates of pixels located on the edge. As with segments, we use the notation  $\mathcal{P}(E, \mathbf{v})$  for the projection of  $E$  on a direction  $\mathbf{v}$ .

1. **Remove non-diagonal edges:** First, edges outside the diagonal stripe area, as shown in Figure 4(b), are excluded. Secondly, for every edge  $E$ , compute the spread of the projections  $s_d = |\mathcal{P}(E, \mathbf{v}_d)|$  and  $s_o = |\mathcal{P}(E, \mathbf{v}_d^c)|$ . Recall that  $\mathbf{v}_d$  is the diagonal direction and  $\mathbf{v}_d^c$  is its orthogonal direction. Based on the ratio  $s_d/s_o$ , we compute an approximation for the orientation of edge  $E$ . Edges well aligned with the diagonal line will yield a large value of  $s_d/s_o$ , while edges well off the diagonal line will have a small value. We filter out non-diagonal edges by requiring  $s_d/s_o \geq \zeta$ . The choice of  $\zeta$  will be discussed later.
2. **Merge edges:** After removing non-diagonal edges, short edges along the diagonal direction are merged into longer edges. The merging criterion is similar to the proximity rule used for diagonal segments. Two edges are merged if their projections onto the diagonal line are close to each other but not excessively overlapped.
3. **Examine prominence:** For edges formed after the merging step, we check their spread along the diagonal direction. An edge  $E$  is taken as a diagonal visual element if  $|\mathcal{P}(E, \mathbf{v}_d)| \geq \xi$ , where  $\xi$  is a threshold to be described next.

The values of thresholds  $\zeta$  and  $\xi$  are determined by the size of a given image.  $\zeta$  is used to filter out edges whose orientations are not quite diagonal, and  $\xi$  is used to select edges that spread widely along the diagonal line. We use the third points on the borders of the image plane to set bounding conditions. Figure 4(c) shows two lines marking the angular range allowed for a nearly diagonal direction from the upper left corner to the lower right corner. Both lines in the figure are off the ideal diagonal direction to some extent. Let  $\zeta_1$  and  $\zeta_2$  be their ratios of  $s_d$  to  $s_o$ , and  $\xi_1$  and  $\xi_2$  be their spreads over the diagonal line. The width and height of

the image are denoted by  $w$  and  $h$ . By basic geometry, we can calculate  $\zeta_i$  and  $\xi_i$ ,  $i = 1, 2$ , using the formulas:

$$\zeta_1 = \frac{h^2 + 3w^2}{2hw}, \quad \zeta_2 = \frac{3h^2 + w^2}{2hw}$$

$$\xi_1 = \frac{h^2 + 3w^2}{3\sqrt{h^2 + w^2}}, \quad \xi_2 = \frac{3h^2 + w^2}{3\sqrt{h^2 + w^2}}.$$

The thresholds are then set by  $\zeta = \min(\zeta_1, \zeta_2)$ ,  $\xi = \min(\xi_1, \xi_2)$ .

## 2.4 “Horizontal”, “Vertical” and “Centered” Composition Types

Now we present our method for differentiating the last three composition categories: “horizontal”, “vertical” and “centered”. Photographs belonging to each of these categories have distinctive spatial layouts. For instance, a landscape with blue sky at the top and field at the bottom conveys a strong impression of horizontal layout. Images from a particular category usually have some segments that are characteristic of that category, e.g., a segment lying laterally right to left for “horizontal” photographs, and a homogeneous background for “centered” photographs.

In order to quantitatively characterize spatial layout, we define the *spatial relational vector (SRV)* of a region to specify the geometric relationship between the region and the rest of the image. The spatial layout of the entire image is then represented by the set of SRVs of all the segmented regions. The dissimilarity between spatial layouts of images is computed by the IRM distance (Li et al. 2000). Ideally we want to describe the spatial relationship between each semantically meaningful object and its surrounding space. However, object extraction is inefficient and extremely difficult for photographs in general domain, regions obtained by image segmentation algorithms are used instead as a reasonable approximation. Moreover, for painters, reducing the complicated appearance into simple masses is a necessary step in her composition, and expresses the “essence” of a painting’s structure (Speed 1972).

### 2.4.1 Spatial Relational Vectors (SRV)

The SRV is proposed to characterize the geometric position and the peripheral information about a pixel or a region in the image plane. It is defined at both pixel-level and region-level. When computing the pixel-level SRV, the pixel is regarded as the reference point, and all the other pixels are divided into 8 zones by their relative positions to the reference point. If the region that contains the pixel is taken into consideration, SRV



is further differentiated into two modified versions, inner SRV and outer SRV. The region-level inner (outer) SRV is obtained by averaging pixel-level inner (outer) SRVs over the region. Details about SRV implementation will be given immediately. As we will see, SRV is scale-invariant, and depends on the spatial position and the shape of the segment.

At a pixel with coordinates  $(x, y)$ , 4 lines passing through it are drawn. As shown in Figure 5(a), the angles between adjacent lines are equal and stride symmetrically over the vertical, horizontal,  $45^\circ$  and  $135^\circ$  lines. We call the 8 angular areas of the plane “UPPER”, “UPPER-LEFT”, “LEFT”, “BOTTOM-LEFT”, “BOTTOM”, “BOTTOM-RIGHT”, “RIGHT”, and “UPPER-RIGHT” zones. The SRV of pixel  $(x, y)$  summarizes the angular positions of all the other pixels with respect to  $(x, y)$ . Specifically, we calculate the area percentage  $v_i$  of each zone,  $i = 0, \dots, 7$ , with respect to the whole image and construct the pixel-level SRV  $V_{x,y}$  by  $V_{x,y} = (v_0, v_1, \dots, v_7)^t$ .

The region-level SRV is defined in two versions called respectively inner SRV, denoted by  $V'$ , and outer SRV, denoted by  $V''$ . At any pixel in a region, we can divide the image plane into 8 zones by the above scheme. As shown in Figure 5(b), for each of the 8 zones, some pixels are inside the region and some are outside. Depending on whether a pixel belongs to the region, the 8 zones are further divided into 16 zones. We call those zones within the region as inner pieces and those outside as outer pieces. Area percentages of the inner (or outer) pieces with respect to the area inside (or outside) the region form the inner SRV  $V'_{x,y}$  (or outer SRV  $V''_{x,y}$ ) for pixel  $(x, y)$ .

The region-level SRV is defined as the average of pixel-level SRVs for pixels in that region. The outer SRV  $V_R''$  of a region  $R$  is  $V_R'' = \sum_{(x,y) \in R} V_{x,y}'' / m$ , where  $m$  is the number of pixels in region  $R$ . In practice, to speed up the calculation, we may subsample the pixels  $(x, y)$  in  $R$  and compute  $V_R''$  by averaging over only the sampled pixels. If a region is too small to occupy at least one sampled pixel according to a fixed sampling rate, we will compute  $V_R''$  using the pixel at the center of the region.

We use the outer SRV to characterize the spatial relationship of a region with respect to the rest of the image. Then an image with  $N$  segments  $R_i, i = 1, \dots, N$ , can be described by  $N$  region-level outer SRVs,  $V_{R_i}'', i = 1, \dots, N$ , together with the area percentages of  $R_i$ , denoted by  $w_i$ . In summary, an image-level SRV descriptor is a set of weighted SRVs:  $\{(V_{R_i}'', w_i), i = 1, \dots, N\}$ . We call this descriptor the *spatial layout signature*.

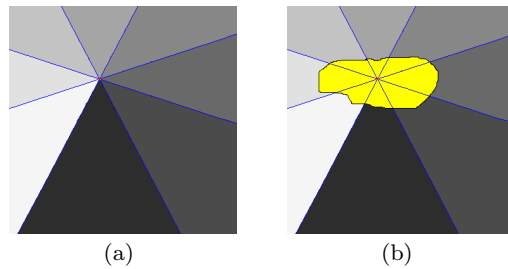


**Fig. 5** Division of the image into 8 angular areas with respect to a reference pixel.

#### 2.4.2 “Horizontal”, “Vertical” and “Centered” Composition Classification

We use k-NN to classify the three composition categories: “horizontal”, “vertical” and “centered”. Inputs to the k-NN algorithm are the spatial layout signatures of images. The training dataset includes equal number of manually labeled examples in each category. In our experiment, the sample size for each category is 30. The distance between the spatial layout signatures of two images is computed using the IRM distance. The IRM distance is a weighted average of the distances between any pair of SRVs, one in each signature. The weights are assigned in a greedy fashion so that the final weighted average is minimal. Details about IRM are referred to Li et al. (2000); Wang et al. (2001).

### 2.5 Composition Sensitive Image Retrieval

The classic approach taken by many image retrieval systems is to measure the visual similarity based on low-level features. A large family of visual descriptors have been proposed in the past to characterize images from the perspectives of color, texture, shape, etc. However, due to the fact that many visual descriptors are generated by local feature extraction processes, the overall spatial composition of the image is usually lost. In semantic content oriented applications, spatial layout information of an image may not be critical, but for photography, the overall spatial composition can be a major factor affecting how an image is perceived. For photographers, it can be more interesting to search for photos with similar composition style rather than visual details. We develop algorithms to capture strong compositional elements in photos and classify them into six composition categories, with five main categories namely “textured”, “horizontal”, “vertical”, “centered”, and “diagonal”, and the “diagonal” category is further subdivided into two categories “diagonal\_ulbr”(upper left to bottom right) and “diagonal\_urbl”(upper right to bottom left). The composition classification is used

in the retrieval system to return images with similar composition.

We use the SIMPLIcity system to retrieve images with similar visual content, and then re-rank the top  $K$  images by considering their spatial composition and aesthetic scores. SIMPLIcity is a semantic-sensitive region based image retrieval system. IRM is used to measure visual similarity between images. For a thorough description of algorithms used in SIMPLIcity, readers are referred to Wang et al. (2001). In our system, the rank of an image is determined by three factors: visual similarity, spatial composition categorization, and aesthetic score. Since these factors are of different modality, we use a ranking schema rather than a complicated scoring equation.

Given a query, we first retrieve  $K$  images through SIMPLIcity, which gives us an initial ranking. When composition is taken into consideration, images with the same composition categorization as the query will be moved to the top of the ranking list.

The composition classification is non-exclusive in the context of image retrieval. For instance, a “textured” image can still be classified into “horizontal”, “vertical” or “centered”. We code the classification results obtained from the classifiers by a six-dimensional vector  $c$ , corresponding to six categories (“diagonal” has two subcategories “diagonal\_ulrb” and “diagonal\_urbl”). Each dimension records whether the image belongs to a particular category, with 1 being yes and 0 no. Note that an image can belong to multiple classes generated by different classifiers. The image can also be assigned to one or more categories among “horizontal”, “vertical” and “centered” if neighbors belonging to the category found by k-NN reach a substantial number (currently  $k/3$  is used). Non-exclusive classification is more robust than exclusive classification in practice because a photograph may be reasonably assigned to more than one compositional category. Non-exclusive classification can also reduce the negative effect of misclassification into one class. Figure 6 shows example pictures that are classified as more than one category.

The compositional similarity between the query image and another image can be defined as

$$s_i = \sum_{k=0}^3 I(c_{q_k} = c_{i_k} \text{ and } c_{q_k} = 1) \\ + 2 \times \sum_{k=4}^5 I(c_{q_k} = c_{i_k} \text{ and } c_{q_k} = 1),$$

where  $c_q$  and  $c_i$  are categorization vectors for the query image and the other image, and  $I$  is the indicator function returning 1 when the input condition is true, 0 otherwise. The last two dimensions of the categoriza-

tion vector correspond to the two diagonal categories. We multiply the matching function by 2 to encourage matching of diagonal categories in practice. Note that the value of  $s_i$  is between 0 and 6, because one image can at most be classified into 5 categories, which are “textured”, “diagonal\_ulbr”, “diagonal\_urbl” and two of the other three. Therefore by adding composition classification results, we divide the  $K$  images into 8 groups corresponding to compositional similarity from 0 to 7. The original ranking based on visual similarity remains within each group. When aesthetic rating is further introduced into the ranking schema, images within each group are reordered by aesthetic ratings. Let  $r_i$ ,  $s_i$  and  $q_i$  denote the rank, compositional similarity, and aesthetic score of image  $i$ . The ranking schema can be expressed as:

$$r_i < r_j \text{ if } \begin{cases} s_i > s_j \\ q_i > q_j, s_i = s_j \end{cases}.$$

The reason we use such a ranking scheme is that we need to incorporate three perspectives of different modalities and it is difficult to put these distinct measurements in the same space. Although the composition analysis is performed on the results returned by a CBIR system SIMPLIcity, we can modify the influence of this component in the retrieval process by adjusting the number of images  $K$  returned by SIMPLIcity. This provides flexibility for the user to vary her focus on either composition or visual similarity. For example, a large  $K$  will retrieve more compositionally relevant photographs, and meanwhile reduce the importance of content similarity. In our experiment, we found that in most cases the retrieved results become stable for our dataset when  $K > 300$ , a value expected to vary with the size of dataset. In Figure 7 we provide some examples showing how different values of  $K$  can affect the retrieved results.

### 3 Color Feedback

Most of the time what people view and perceive from photos is through colors. Although people’s feeling about colors may depend on many factors such as context, emotion, culture background, etc., there are some color combinations or arrangements considered to be perceptively stable (Manav 2007; Gao et al. 2007). Experienced photographers can choose specific color combinations to enhance viewers’ emotion and to achieve an aesthetically pleasing perception. The study of color and light can be traced back to as early as seventeenth century when Isaac Newton invented the first color wheel. The foundations of modern color theory were laid at the

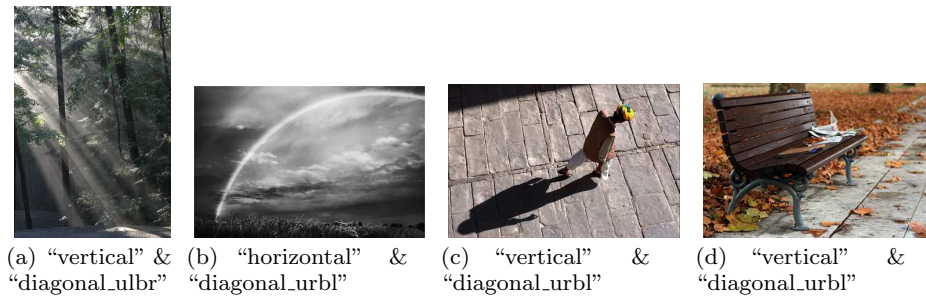


**Fig. 6** Photographs classified into multiple categories. “diagonal\_ulbr” represents the diagonal from the upper left corner to the bottom right corner, and “diagonal\_urbl” represents the other.

beginning of the twentieth century. Itten (1960) introduced a new color wheel with emphasis on hue information. He proposed several color harmony schemes, such as complementary color harmony, three-color harmony of hues forming an equilateral triangle, four-color harmony of a square, etc., which have been widely adopted by artists and designers. Tokumaru et al. (2002) used 80 color schemes for harmony evaluation and color design and proposed an approach to quantify human’s perception and understanding about color combinations. Recently, research efforts have been devoted to improving the visual appeal of an image by enhancing the harmony among colors under an optimization framework (Cohen-Or et al. 2006). In this paper, we propose a data driven approach to assess the qualities of color combinations. Our color feedback module can quickly extract the color palette of a photo and tell photographers if these color combinations are aesthetically appealing. The colors are specified completely with hue, saturation intensity, and luminance value rather than only by hue.

We first segment each image by a recently developed clustering technique, i.e., hierarchical mode association clustering (HMAC) (Li et al. 2007). Our image segmentation approach consists of the following steps: (a) Apply k-center algorithm to cluster pixels into a fixed number of groups. This number is significantly larger than the desired number of segments. In particular, we set it to 100. (b) Form a data set  $\{x_1, \dots, x_n\}$ ,  $n = 100$ , where  $x_i$  is the mean of the vectors assigned to group  $i$  by k-center clustering. Assign weight  $w_i$  to each group  $i$ , where  $w_i$  is the percentage of pixels assigned to that group. (c) Apply HMAC to the data set. Specifically, the kernel density estimator of modal clustering is  $f(x) = \sum_{i=1}^n w_i \phi(x|x_i, D(\sigma^2))$ , where  $\sigma$  is the *bandwidth* of the Gaussian kernel and  $D(\sigma^2) = \text{diag}(\sigma^2, \sigma^2, \dots, \sigma^2)$ . All the data points that ascend to the same local maximum (mode) of the kernel density function form a cluster. (d) In the dendrogram formed by HMAC, we apply the cluster merging algorithm described in Li et al. (2007). If the number of clusters

after merging is smaller than or equal to the given target number of segments, stop and output the clustering results at this level. Otherwise, repeat the merging process at the next higher level of the dendrogram. Finally, all the pixels in the same cluster are labeled as one segment.

After segmentation, all the modal vectors are extracted as the representative colors of that image. K-means clustering is another widely used image segmentation method, which clusters the pixels and computes the centroid vectors by minimizing the mean squared distance between the original vectors and the centroid vectors. HMAC, however, uses the modal vectors, at which the kernel density estimator achieves a local maximum. These vectors are peaks of the density function. The representative colors extracted by k-means are often “muddy” due to averaging, while those by modal clustering better retain the true colors. When the number of segments is set to a higher value, the representative colors obtained by modal clustering tend to be more saturated. In particular, we set the target number of clusters to 15, a fairly large value, so that the modal color vectors will not miss any local maximum of the density. If some segment only occupies a small percentage of all the pixels, specifically, less than 5%, its color will be ignored. After the representative colors are obtained by HMAC, we form color triplets by combining every three distinct colors from that image. For instance, if one image contains  $n$  representative colors, there will be  $n(n-1)(n-2)/6$  color triplets (aka combinations). In practice, if there are many colors in one image, we will only consider the representative colors of the five largest segments. We provide feedback in the form of color triplets because the triplet is a good balance for capturing the diversity in color combination and maintaining manageable complexity for human cognition. In fact, in many photography or painting books about color composition, good color schemes are often described by no more than three major hues (a variation range allowed for each hue). Technically, the

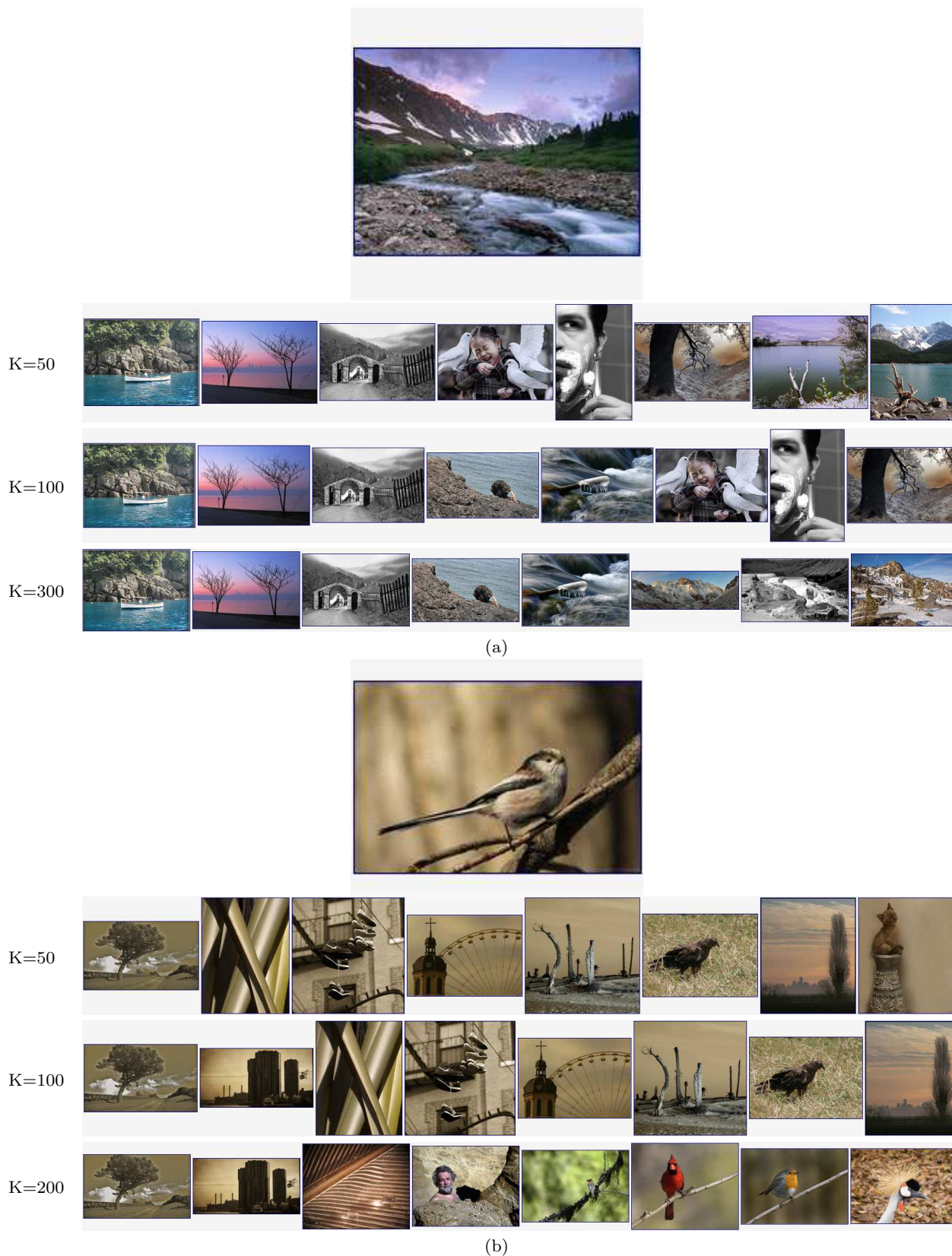


**Fig. 7** Images retrieved by different values of  $K$ , using composition categorization to rerank results returned by SIMPLiCity. (a) The query image is at the top center and top 8 re-ranked images retrieved when  $K = 50$ ,  $K = 100$  and  $K = 300$  are shown in three rows; (b) A second example with the query image at the top center and the top 8 re-ranked images retrieved when  $K = 50$ ,  $K = 100$  and  $K = 200$  are shown in three rows.

probability of finding a combination of frequent color quadruplet is lower than finding a frequent color triplet among the highly rated images. To gain high confidence level for a quadruplet, if necessary, a much larger set of high aesthetic quality images are needed.

Let us denote a color triplet  $\beta_i$  by  $(v_i^{(1)}, v_i^{(2)}, v_i^{(3)})$ , where  $v_i^{(j)}$  is a color vector,  $j = 1, 2, 3$ . Let  $q_i^{(j)}$  be the weight of each color vector  $v_i^{(j)}$ , i.e., the percentage of occupied pixels by a particular color.  $q_i^{(j)}$  is normalized so that  $\sum_{j=1}^3 q_i^{(j)} = 1$ . The Kantorovich-Mallows distance (Mallows 1972; Levina and Bickel 2001), which takes into account the relative area size covered by each color, is used to compute the distance  $D(\beta_1, \beta_2)$  between two color triplets  $\beta_1$  and  $\beta_2$ :

$$D^2(\beta_1, \beta_2) = \min_{w_{i,j}} \sum_{i=1}^3 \sum_{j=1}^3 w_{i,j} \|v_1^{(i)} - v_2^{(j)}\|^2 \quad (1)$$

subject to

$$\begin{aligned} \sum_{j=1}^3 w_{i,j} &= q_1^{(i)}, i = 1, 2, 3; \\ \sum_{i=1}^3 w_{i,j} &= q_2^{(j)}, j = 1, 2, 3; \end{aligned} \quad (2)$$

$$w_{i,j} \geq 0, i = 1, 2, 3, j = 1, 2, 3.$$

The Kantorovich-Mallows distance has been used in content-based image retrieval, mostly under the name of *Earth Mover's Distance (EMD)* (Rubner et al. 2000). It was proved by Levina and Bickel (2001) that EMD is equivalent to the Kantorovich-Mallows distance on probability distributions. When measuring texture and color similarities for image retrieval, EMD is more robust than norm distances since it can be applied to variable-length representations of distributions (Rubner et al. 2000).

We use k-NN to evaluate the aesthetic qualities of color combinations. Specifically, we form the training data by collecting all the valid color triplets described above from images with high aesthetic ratings as well as those with low aesthetic ratings. We assume that all the color triplets from high rating images are aesthetically pleasing, which are called highly aesthetic triplets. Given a color triplet from a test image, we first find the top  $k$  nearest color triplets in the training data. Then, the percentage of highly aesthetic color triplets are calculated. We refer to this percentage as the *ratio statistic* of a color triplet, denoted by  $\gamma$ . A *p-value* is defined on the ratio statistics, indicating our confidence about the goodness of a color triplet. Specifically, we first obtain the ratio statistics of all the high aesthetics color triplets from the training data, denoted by  $\{\gamma_1, \gamma_2, \dots, \gamma_n\}$ , where  $n$  is the total number of highly

aesthetic triplets. Suppose the ratio statistic of a particular color triplet from a test image is  $\gamma$ . Its p-value is defined as the percentage of highly aesthetic triplets in the training set whose  $\gamma_i$ 's are larger than  $\gamma$ , i.e.,  $\sum_{i=1}^n I(\gamma_i > \gamma)/n$ , where  $I$  is an indicator function. If a color triplet's p-value is small, we have strong confidence that it is of high aesthetic quality. To make p-value more straightforward to use, we define a confidence score as  $100(1 - p)$ .

The underlying assumption that all the color combinations from photos with high aesthetic ratings are aesthetically pleasing is debatable. One may argue that a photo may be appealing due to visual qualities other than colors. This concern can be addressed effectively in the future because we are employing the ACQUINE system to collect users' opinions on why a photo is aesthetically appealing; and one choice among many is color scheme. After we have collected sufficient amount of data, we can choose images with high aesthetic scores resulting from colors as our training data. On the other hand, we should be cautious that doing so may restrict our findings about good color schemes to the common knowledge the general public holds. A viewer may be subconsciously attracted to some color combinations. As a result, she may give the photo high aesthetic rating but not realizing that the colors have played a role. For instance, even painters often do not realize the beauty brought by neutral (aka grays of various hues) colors and the importance of using neutral colors to the advantage. According to Robert Henri, a renowned artist and art educator (Henri 1923), "But even so, there is a power in the palette which is composed of both pure and grave colors that makes it wonderfully practical and which presents possibilities unique to itself. In paintings made with such a palette, if used with great success, we find an astounding result. It is the grave colors, which were so dull on the palette that become the living colors in the picture. The brilliant colors are their foil." Further, Henri mentioned that grave colors "seem to move—rise and fall in their intensity, are in perpetual motion—at least, so affect the eye. They are not fixed. They are indefinable and mysterious."

## 4 Aesthetic Feedback

In this section we introduce the component of aesthetic quality feedback on both color and monochromatic images. We assign aesthetic ratings to images on a scale of 0 to 100 based on the models learnt using previously rated images. An on-line demo-version of this component can be found at [acquine.alipr.com](http://acquine.alipr.com) which derives visual features to quantify the general photography principles and has been discussed in detail by

Datta et al. (2006). Our main contribution to this component lies in the addition of a model specific to analyze the aesthetics of monochromatic images. Though the demo is one of its kind to predict the aesthetic ratings reliably in real-time, its accuracy falters in the case of black and white images. This is due to the primary differences in the aesthetic rules of color and monochromatic images.

Unlike the color images whose aesthetics are highly influenced by their color distribution, the black and white images are subtle in their appearance. The black and white images are less distracting than their colored counterparts, they are very simplistic in nature and lay emphasis on the subject. The photographer needs to provide great attention to the image composition and develop emotions through careful manipulation of the tonality in the image. It becomes essential to imply color through contrasts making black and white images more artistic as well as challenging at the same time (Davis 2010; Taylor et al. 2000). The shape (the two dimensional outline of an object), design and form (the perceived rendering of a three dimensional object in two dimensional space) of the subject gains prominence in black and white images. The subject of the photograph needs to be located on the salient regions in order to attract immediate attention of the viewer. The lighting of the subject, the balance of elements within the image becomes an integral part of its composition. Some of the well known famous photographs are actually taken in black and white showing its superiority in aesthetics. To draw the comparison between color and gray scale image aesthetics the Figure 8 shows a color image of a red tulip, the saturated red of the tulip and its contrasting background makes the image look attractive while the grayscale representation of the same looks much more drab since it lacks contrast and its corresponding aesthetic rating would be low. This is a perfect example which shows the importance of contrast manipulation, choosing a good subject, its lighting, the background color (negative spaces) for a grayscale image. A detailed analysis of aesthetic primitives and their influence can be found in Peters (2007).

Previous works (Datta et al. 2006; Ke 2006; Luo and Tang 2008; Wong and Low 2009) on image aesthetics have developed generic models by using images rated on [photo.net](http://photo.net), [dpchallenge.com](http://dpchallenge.com) or Flickr. Black and white images formed a very small fraction of these datasets. The general population prefers to take photographs in color leaving the black and white images to professionals who take aesthetically pleasing images. The models learnt on such a dataset using data driven approaches will be biased towards assigning black and white images a very high score. This is due to the lack of a uniformly

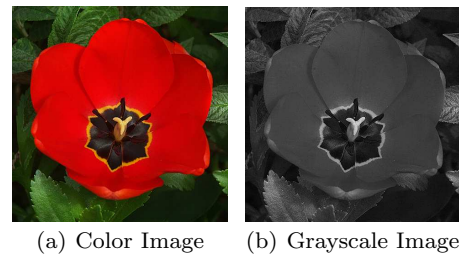


**Fig. 8** Comparison between Color and Grayscale Image Aesthetics.

sampled dataset as well as the over simplification of composition rules which plays a very important role in the aesthetics of black and white images. This led us to seek better datasets which show consensus on the ratings and provide wider score range.

We evaluate the visual features extracted to quantify the aesthetics and photo quality by doing a simple classification between images which have high and low ratings using Support Vector Machines (SVM). Having verified our hypothesis on aesthetic rules, we go on to build a regression model using linear regression which can provide a machine generated aesthetic quality rating for any black and white image. We briefly describe the dataset below and go on to provide detailed description of the visual features.

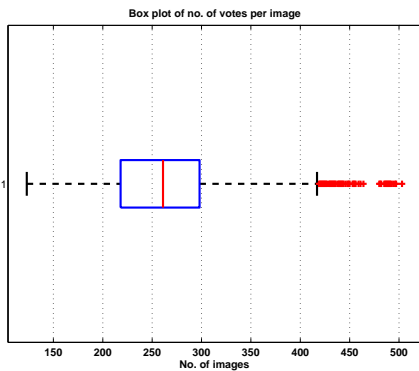
#### 4.1 Dataset

To understand the general consensus of general population on the aesthetics of black and white images, we crawled the website of [www.dpchallenge.com](http://www.dpchallenge.com), a digital photography contest website for the purpose of data collection. [Dpchallenge.com](http://dpchallenge.com) hosts contests with specific themes which are open for a limited number of days. The members of this community are expected to vote on at least 20% of the images on the scale of 1-10 for their votes to be counted. This inadvertently leads to a large number of votes per image and the same time introduces noise due to the fatigue of voting a large number of images continuously and due to the users tendency to assign similar scores to images.

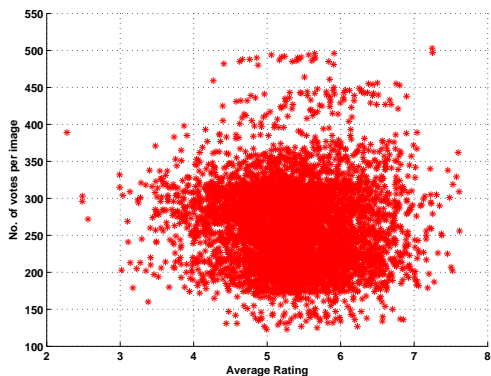
We collected images totaling 8,470 of which 5,790 had ratings. It is observed from our dataset that on an average each image has been rated 262 times with the score range and variance of 5.34 and 0.486 respectively. Some of the sample images from the dataset as well as the score distribution against the number of votes are shown in Figure 9.



(a) Avg. Rating: 2.562 (b) Avg. Rating: 5.720 (c) Avg. Rating: 7.041



(d) Box plot of no. of votes



(e) Average rating vs no. of votes

**Fig. 9** Sample images and score distribution of images from dpchallenge.com.

#### 4.2 Visual Features for Black and White Images

In addition to adopting a few features from Datta et al. (2006), we developed newer features focused on extracting local contrast, details, shapes and saliency.

#### 4.3 Global and Local Sharpness

Sharpness of the image is an indicator of its clarity and detail, in professional photographs one would expect the subject of the photograph to be sharp and most often there is a contrast between the sharpness of the subject and its background leading the viewer's eye on to the subject. Computationally the sharp segments can

be detected by the density of the edges and texture content. In order to extract this information we quantify both the local and global sharpness of the image. If the focal length is set to maximum, the entire image will be in focus while setting the focal length to minimum causes the entire image to be out of focus and is aesthetically displeasing which can be captured by the global sharpness measure ( $S_g$ ). High frequency components indicate the presence of edges and in turn the sharpness. We perform three level Haar Wavelet Transform to extract the high frequency components in each level namely  $LH_i, HL_i, HH_i$  where  $i = 1, 2, 3$ . We store the global sharpness information as

$$S_{gi} = \frac{1}{S_i} \left\{ \sum_{(x,y)} \|w_i^{hh}\| + \sum_{(x,y)} \|w_i^{hl}\| + \sum_{(x,y)} \|w_i^{lh}\| \right\},$$

where  $S_i = |w_i^{hh}| + |w_i^{hl}| + |w_i^{lh}|$  as implemented in Datta et al. (2006).

However in low depth of field images, the subject of the photograph might occupy a very small fraction of the image and the global sharpness measure might mislead us to conclude that the image is entirely out of focus. In order to prevent this, we devised a local sharpness measure ( $S_l$ ) which calculates sharpness within the image segments  $\{s_1, s_2, s_3, \dots\}$  of areas  $\{a_1, a_2, a_3, \dots\}$ , generated by the agglomerative segmentation algorithm (Li 2011). Since the number of segments generated by the unsupervised algorithm is uneven, we store the area of the image which has at least 80% of the total sharpness in level three of Haar Wavelet Co-efficients as a feature. We also store the ratio of minimum number of segments which results in 80% of the sharpness in the image, i.e.  $\{\text{Min no. of segments with cumulative sharpness of 80\%} / \text{total no. segments in the image}\}$ . The normalized area and its centroid of the segment with the maximum sharpness are also stored as features.

In addition to these features, we implement another global blur detection algorithm from Tong et al. (2006) and store the blur confidence co-efficient of the image.

#### 4.4 Image Tonality and Contrast

As opposed to color images, black and white images do not possess vibrant colors and the photographer must induce various levels of tonality and contrast to the image in order to bring strong emotions, detail and perspective into the picture. In a high key image, the light tones predominate which depicts emotions of energy, happiness and life while in a low key image the dark tones predominate portraying lifelessness, dullness and a general negativity. Dark blacks, bright whites, subtle

shadows, smooth tonal transitions without posterization or noise, highlights that are not blown out are some of the good tonal characteristics of Black and White Images (Suess 1995).

The above characteristics can be captured by carefully studying the image histogram, we split the image histogram into three regions defining low-key region between 0-85 , mid-key region between 86-170 and high-key region between 170-256. We analyze these sub-histograms and store their corresponding means and variances which can capture the contrast as well as detect the tonality of the image. Figure 10 shows examples of low, mid and high key images.

We also store the shortest range and the mean of the histogram which accounts for the 90% of the mass of the image. This feature helps in defining the contrast across the image.

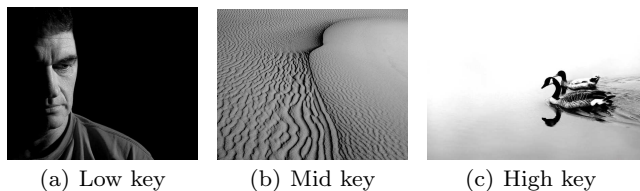


**Fig. 10** Variation in image tonality.

#### 4.5 Convex hull and Normalized Inertia

The shapes and forms are some of the primary composition elements of black and white photographs. Though it is easier to understand and represent shapes, identifying the forms of objects is a very hard problem computationally. We try to approach this problem with the assumption that careful positioning of convex and circular shapes in the image can generate higher aesthetic impact. In order to find the convex shapes in the images we use the feature derived from Datta et al. (2006).

The convexity of the image is represented as the ratio of the area of the convex segments to that of the image area. A segment can be considered convex if its convex hull is closer to its area on the image. Hence the convex Area =  $\sum_i I [a_i / convexHull(s_i) > 0.8] a_i$  where  $s_i$ ,  $a_i$  and  $I$  are the image segment  $i$ , segment area and the indicator function respectively. The convexity feature is limited by the segmentation algorithm. One of the many reasons we use connectivity constrained agglomerative clustering is to prevent over segmentation of objects in the image. The results presented in Li (2011) shows that the algorithm is able to generate clear segmentation generally without breaking up the

object in which case the convexity of the object holds true. On the other hand a convex object could be over segmented into many non-convex and convex segments in which case the convexity of the individual segments do not add up to the convexity of the object, which is an artifact of this feature.

We also describe the circularity of shapes using normalized inertia (Gersho 1979). The discrete form of normalized inertia of order  $\gamma$  for the segment  $s_i$  is represented as

$$N(s_i, \gamma) = \frac{\sum_{x \in s_i} \|x - \bar{x}_i\|^\gamma}{a_i^{1+\frac{\gamma}{2}}}. \quad (3)$$

Since normalized inertia is invariant to scale and rotational changes, it can be considered as a robust descriptor. Circular shapes achieve the minimum normalized inertia, and hence by calculating the ratio of the normalized inertia of segment to that of a circle, we can infer how close the shape of the segment is to a circle. Let  $L(s_i, \gamma)$  be the ratio  $N(s_i, \gamma) / N_c(\gamma)$  for the segment  $s_i$ , where  $N_c(\gamma)$  is the normalized inertia of a circle for the parameter  $\gamma$ . We calculate  $L(s_i, \gamma)$  for  $\gamma = 1, 2, 3, 4, 5$  and store the value  $\sum_{s_i} L(s_i, \gamma)$  for each order  $\gamma$  as a feature.

#### 4.6 Image Saliency

Salient regions in the image are the ones which stand apart from the rest due to their contrast, sharpness and edges. It is highly likely that the viewer would focus his/her attention on the salient region before moving on to other parts of the image. Positioning the subject on salient regions and at the same time positioning the salient regions on the thirds of the image leads to better composition.

To capture this information, we extracted the saliency map of the image using the graph based visual saliency (Harel et al. 2007) which generates a soft saliency map, assigning its confidence on each pixel to be salient. We threshold this saliency map at three levels, 75%, 50% and 25% to extract the image regions which are salient and store the normalized area of these regions as well as their centroids to check the rule of thirds. Figure 11 shows the salient section of the image thresholded at 3 different level.

#### 4.7 Photo Quality - Aspect Ratio and Noise Level

It is known that bad image quality leads to bad aesthetics. We used very intuitive features like the size, aspect



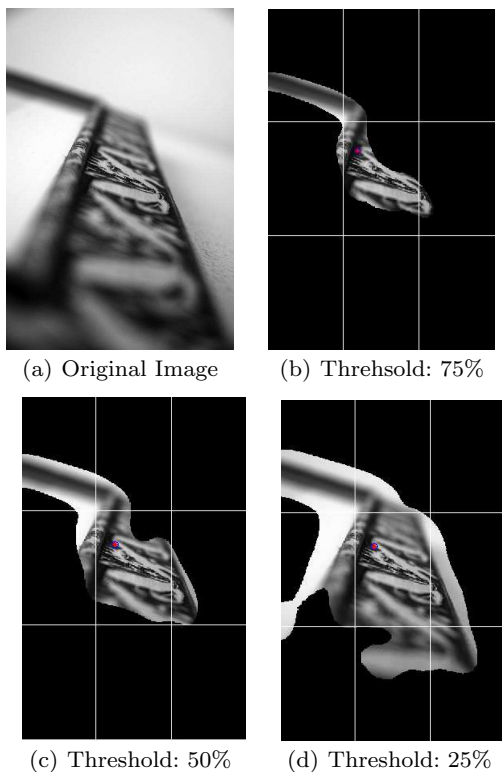


Fig. 11 Salient regions using different threshold levels.

ratio of the image and the noise level in the image to quantify photo quality. The size of the image should add to the beauty of the subject in the picture. A well centered symmetric subject is better framed in a square than in a standard rectangular 4:3 frame.

In order to detect sensor noise and noise added by using high ISO settings which leads to grainy images, we use the noise estimation technique developed by Kisilev et al. (2007). The image is divided into blocks of  $10 \times 10$  and the median absolute deviation from the mean is used to quantize the variance in each of the block. The logic behind this method is to detect the blocks which have the least amount of texture but are inherently noisy at the same time. The mean variance of the top 30 blocks with minimum median absolute deviation is stored as the average noise of the image. Figure 12 shows the variation in the noise level of low and high rated images.

## 5 Experiments

In this section we evaluate individual modules and demonstrate the functions of the OSCAR system. Experimental results for each module will be presented separately. Feedback for example photographs will be shown later.

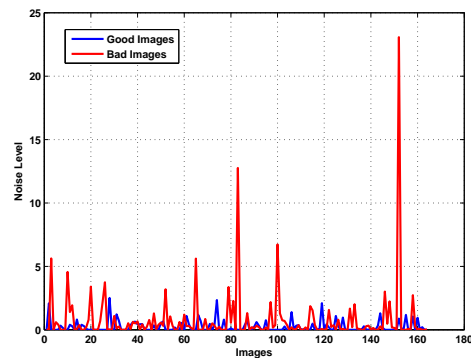


Fig. 12 Noise level comparison between high and low rated images.

### 5.1 Evaluation of Modules

Our system consists of three modules, namely the composition, color feedback, and aesthetics rating modules. Experiments and discussion for each module are presented below.

#### 5.1.1 Composition Module

The composition module analyzes the compositional properties of a photograph. We apply three classifiers to each image, namely the “textured” vs “non-textured” classifier, the diagonal element detector, and the k-NN classifier for “horizontal”, “vertical” and “centered” compositions. The classification can be either exclusive or non-exclusive. We use exclusive classification to evaluate the performance of classifiers, but chose to use non-exclusive classification in the retrieval system. Next we will discuss experimental results in diagonal element detection, and k-NN classification for “horizontal”, “vertical”, and “centered” classes.

*Diagonal Element Detection* Algorithms for detecting diagonal element are provided in Section 2.3. We use both segments and edges as visual cues. After segmentation and edge detection, small segments or edges aligning along the same diagonal direction are merged. These merged segments or edges with wide spread along either of the diagonal lines are marked as diagonal elements. The images which contain diagonal elements are classified into the “diagonal” category.

Figure 13 shows some examples for merging segments or edges. Images in the second column show edges and segments generated by edge detection and image segmentation, where disconnected edges or segments are marked by different colors. The third column contains images displaying the detected diagonal elements after merging. In our experiment, we find that

merging occurs more frequently with edges than segments. This might be caused due to the fact that the long lines are more likely to be broken into disconnected edges (gaps in edge detection) than elongated regions being divided into several segments.

The current algorithm has some of the following limitations. Firstly, diagonally oriented edges in a noisy context (many other edges in the neighborhood) do not emerge as salient visual elements. Merging edges in a noisy context will lead to false identification of diagonal composition. Secondly, the algorithm only merges diagonally oriented edges or segments. Therefore, it cannot detect more subtle diagonal visual paths formed by edges or segments that are not individually oriented in a diagonal fashion.

Some examples of diagonal element detection are given in Figure 14. Images in the first column are the original pictures. The second column and the third column contain image segmentation and diagonal segment detection results, while the last two columns show the edge detection and diagonal edge detection results. Currently, we only provide information about whether a photograph is diagonally composed or not. The system can be enhanced to take requests as to whether a photograph contains near-diagonal elements so that users can be alerted to adjust the frame to achieve a stronger diagonal composition while taking photographs.

*Classification of Spatial Composition Categories “Horizontal”, “Vertical” and “Centered”* We apply k-NN classification algorithm ( $k = 30$ ) on the spatial layout signatures of images using the IRM distance. In the training dataset, the sample size for each category is 30. Figure 15 shows example photos classified as “horizontal”, “vertical” and “centered” by the k-NN classifier. Misclassification can be caused by a biased training dataset because the image samples in the training dataset may not represent sufficiently the corresponding category. Poor segmentation can also lead to misclassification, since the spatial layout signature is sensitive to the image segmentation results. For example, “centered” photographs can be misclassified if the background is incorrectly broken into multiple segments. We notice that the spatial layout signature of a “centered” photo distinguishes itself clearly from “horizontal” and “vertical” signatures when the centered segment, usually the subject, fills a major portion of the image plane. It can also occur when the background segment takes up a major portion of the image plane or when the segments on the boundary region are evenly distributed.

*Confusion Table* In order to evaluate the performance of our composition classification algorithms, we apply

**Table 1** Confusion table for composition classification on 222 images from five categories

	h	v	c	ulbr	urbl
h	44	0	0	3	3
v	0	34	7	8	2
c	6	3	29	5	7
ulbr	0	1	2	30	2
urbl	0	3	0	0	33

the three classifiers on 222 manually labeled photographs, among which 50 are horizontally composed, 51 are vertically composed, 50 are centered, and 71 are diagonally composed (35 have visual elements along the diagonal line from the upper left corner to the bottom right corner, and 36 have diagonal elements in the other direction). Images in the testing dataset are pictures which have composition clarity and fit into single category.

In this experiment, we will perform an exclusive classification. The classifiers are applied on an image sequentially. That is, we first use the “textured” vs “non-textured” classifier to determine whether the image looks “textured”. If this classifier labels it “non-textured”, the diagonal element detector is then applied. Provided any diagonal element is detected, the image is assigned to one of the diagonal categories according to its orientation. If the category of the image is still undetermined, the k-NN classifier finally decides its composition type by classifying it under the category which gets the most votes. We only evaluate the diagonal detector and k-NN classifier for “horizontal”, “vertical” and “centered”, since “textured” vs “non-textured” classifier is not newly developed in this paper. Hence the first step of the above process is skipped in this experiment. We denote these categories by “h” for “horizontal”, “v” for “vertical”, “c” for “centered”, “ulbr” for diagonal direction from the upper left corner to the bottom right corner, and “urbl” for the other. Table 1 gives the confusion table for this testing dataset. More results and discussion on composition classification are provided in Section 6.

### 5.1.2 Color Feedback Evaluation

Our color feedback module is evaluated on the same dataset used in Section 5.1.1 except with all the gray scale images removed. In total, there are 11,241 images, with ratings between 2.33 and 6.90 (out of 7.00). The distribution of these ratings is shown in Figure 16(a). Images with high aesthetic ratings are generally of high quality. For training, we randomly select half of the images with top 5% ratings and half of the images with bottom 5% ratings. HMAC (Li et al. 2007) is used to segment these images. As mentioned in Section 3, the



**Fig. 13** Merging edges or segments to form more prominent diagonal elements. First column: original images; Second column: edge detection or segmentation results; Third column: edges or segments that are merged and identified as diagonal elements.

target number of clusters in HMAC is set to 15, and we extract the 5 most dominant colors from that image if it has more than 5 colors. Then in each image, every three distinct colors form a color triplet, or color combination. The images with fewer than 3 colors will be excluded. All the color triplets from images with top ratings are supposed to have good aesthetics, and are called the highly aesthetic triplets. At the end, we obtain a training dataset containing 1,794 highly aesthetic color triplets and 1,890 triplets from low rating images. K-NN is used to calculate the *ratio statistics* of color triplets, with  $k$  equal to 120.

We first obtain all the ratio statistics of highly aesthetic color triplets as well as the triplets from low rating images, the histograms of which are shown in Figure 16(b) and 16(c). Note that the distribution in Figure 16(c) has two modes, which may indicate that though low rating images are more likely to have color triplets of low aesthetic quality, they may also contain certain good color triplets. Then we calculate all the confidence scores of the color triplets from high quality images in

the training data. The larger the score, the more confidence we have to claim a particular color triplet to be aesthetically pleasing. The color triplet with the largest confidence score within each image is selected, i.e., the one with the highest aesthetics. Then we rank these selected color triplets based on their confidence scores, the one with the largest score on the top. Figure 17 shows the top 20 highly ranked color triplets. Among those color triplets, a few contain colors that have nearly the same hue. The majority of the color triplets contain colors similar in hue. And yet a few triplets contain complementary colors with one hue occupying two colors with different luminance. There is a possibility that a region with smooth while large tone transition in the image is over segmented. On the other hand, purely from the perspective of studying color, it can be useful to divide colors of similar hues but very different tones (i.e. light intensity) into separate regions. Variation in tone but not hue impacts human perception deeply. In art books, artists are often reminded that getting the tone right is more important than getting

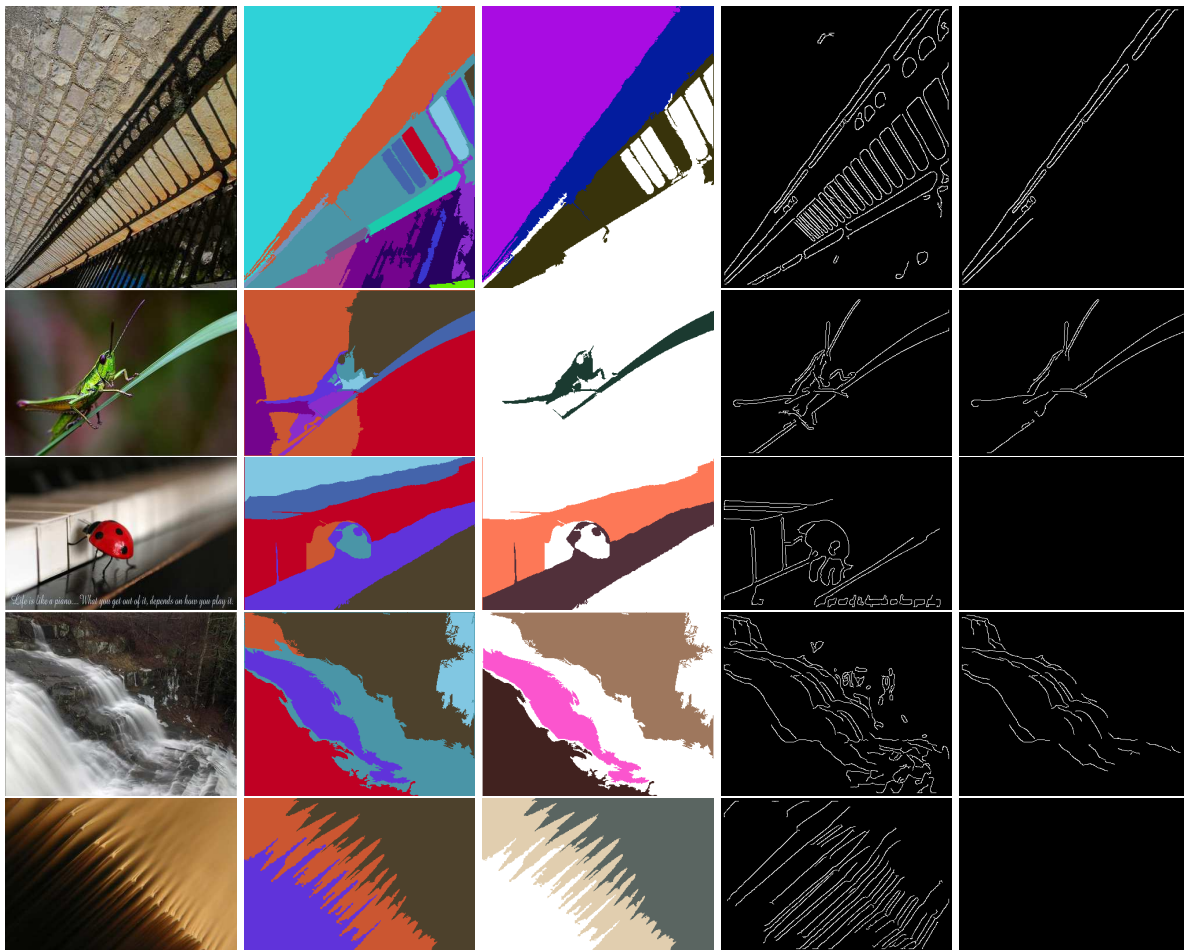


**Fig. 14** Diagonal element detection. First column: original images. Second column: segmentation result. Third column: segments detected as diagonal. The white area covers non-diagonal segments. Fourth column: edge detection result. Fifth column: detected diagonal edges.

the color hue right because the viewer’s impression of the three dimensional world relies largely on the correct relationship in tone rather than in hue. A picture that conveys a strong sense of three dimensions, let it be a painting or a photograph, is usually appealing. In the case of paintings, such works are often marveled at. Additionally, the color triplets found in Figure 17 are not highly saturated, which may be a reflection of Robert Henri’s remarks about the attractiveness of grave colors in pictures (Henri 1923).

We randomly select several images with high, middle, and low ratings, and evaluate the aesthetic qualities of their color combinations using our color feedback module. The color triplet from each image with the largest confidence scores, presumably most aesthetically pleasing color combination, are shown in Figure 18. The number under each image is the corresponding confidence score of the best color triplet chosen. Images with high, middle, and low ratings are shown in the first, second and third row, respectively. As we can

see, the most aesthetically pleasing color triplets from images with high and middle ratings usually have larger confidence scores. This indicates that we are more confident about the aesthetic appeal of these color combinations. However, note that the largest confidence scores of color triplets from Figure 18(d) and Figure 18(k) are 68.5 and 5.4, although these two images receive good ratings. This may indicate that viewers are attracted to these photos by aspects other than color. On the other hand, even though Figure 18(m) has a low rating, it includes a color combination with confidence score as large as 87.7.

### 5.1.3 Black and White Aesthetics Rating

In order to verify the discriminative power of our features we performed classification between images with high and low aesthetic ratings. In order to clearly demarcate the images which have higher aesthetics from the ones with lower aesthetics, we group images above

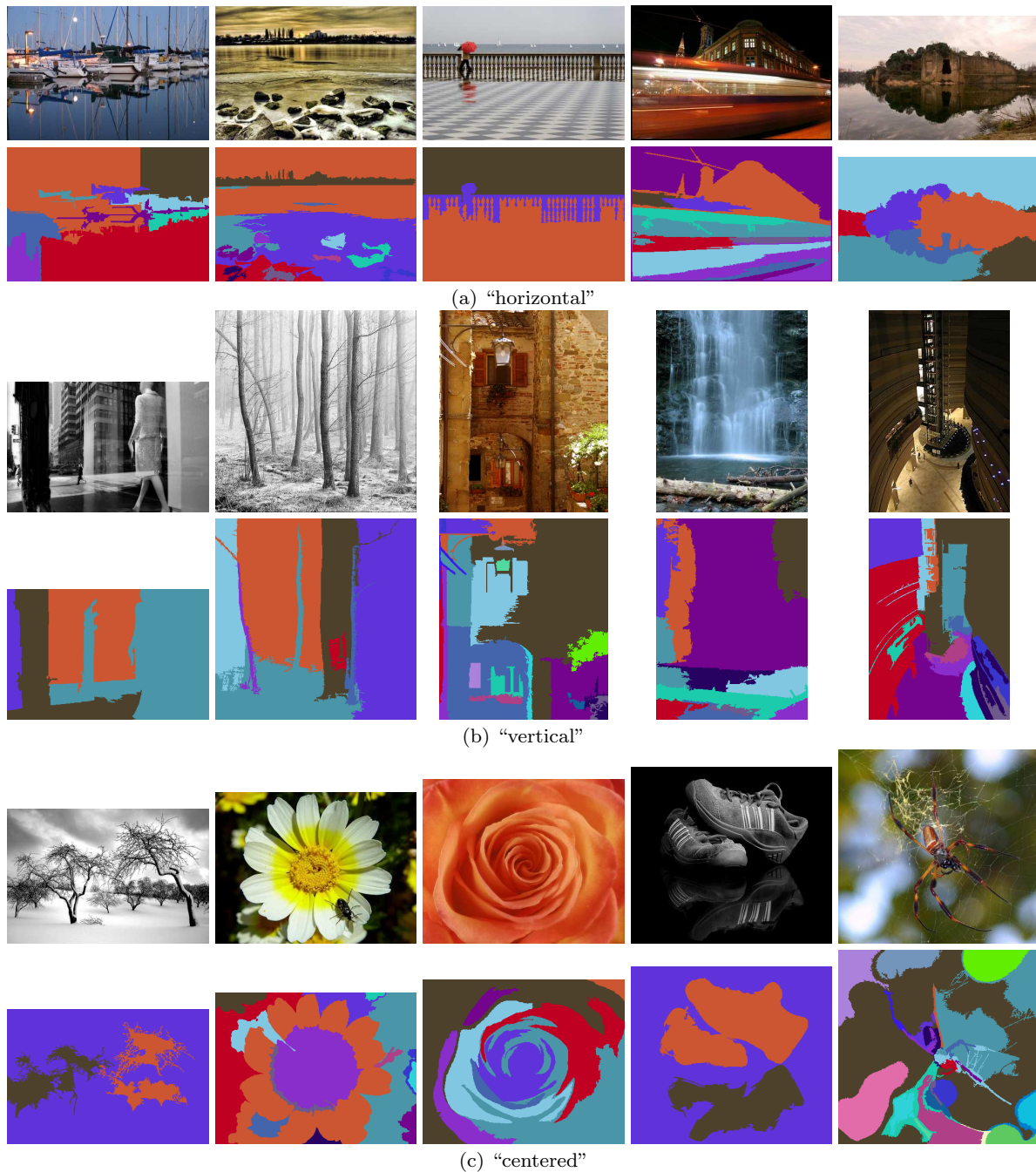


**Fig. 15** Example photos classified as "horizontal", "vertical", and "centered". First row: original images. Second row: segmentation result.

a given threshold as good images and the images below a threshold as bad images. These thresholds are varied to check for classifier performance and robustness. We grouped images with average aesthetic ratings above two thresholds 6 and 6.5 as pleasing while the images with average ratings lower than 5 and 4 as images with bad aesthetic quality.

We extract features detailed in Section 4 from images conforming to the thresholds mentioned above and perform classification using Support Vector Machines. The R implementation of "kernlab" (Karatzoglou 2004) which has an in-built automatic kernel parameter optimizer was used. The table 2 shows the classification results, the average accuracy with and without dimensionality reduction using Principal Component Analysis

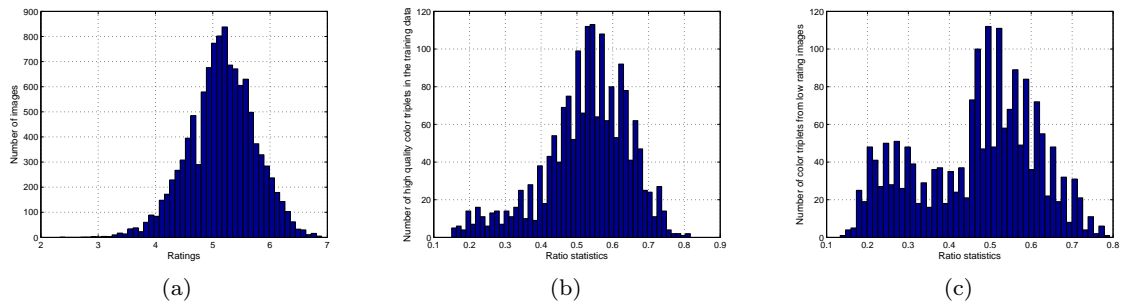


**Fig. 16** (a) Distribution of image ratings; (b) Distribution of ratio statistics for all the high aesthetics color triplets in the training data; (c) Distribution of ratio statistics for color triplets from low rating images in the training data.

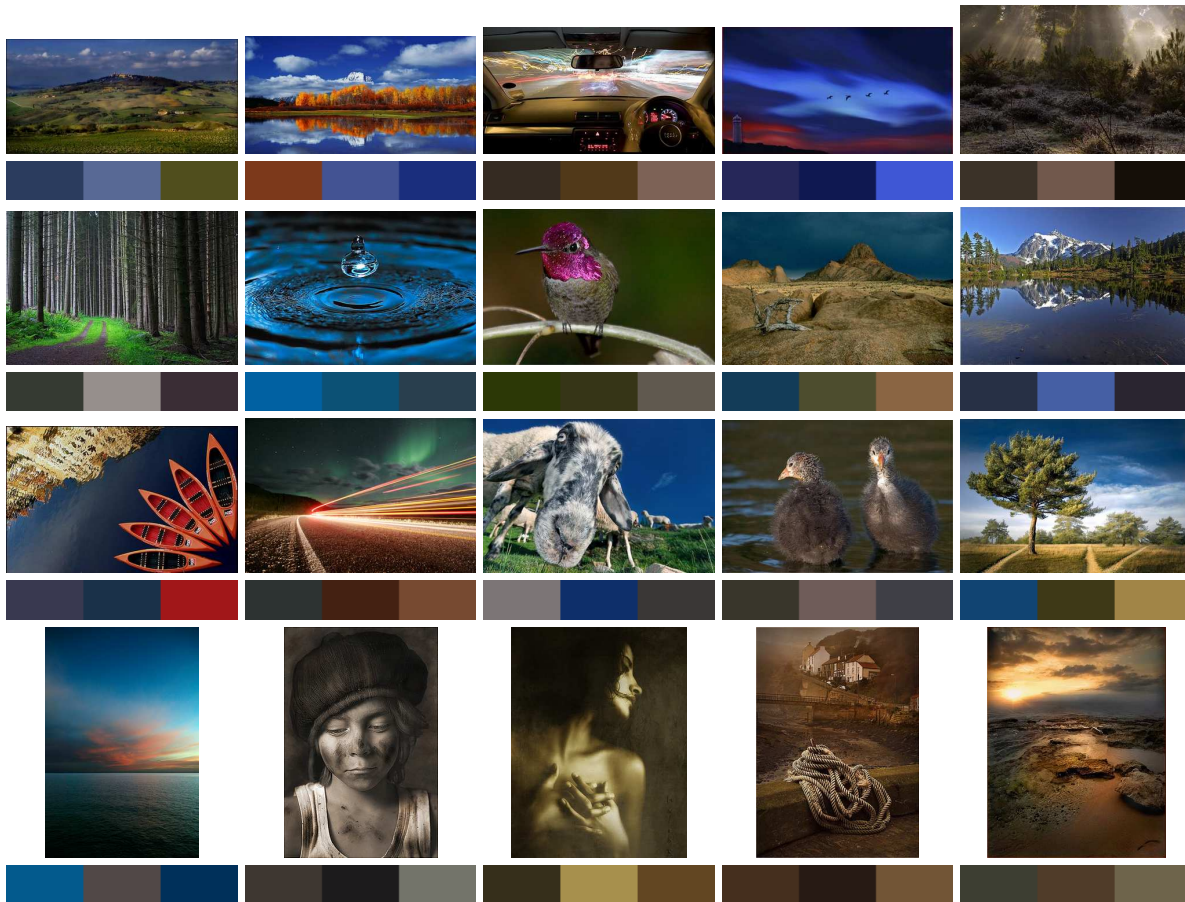


**Fig. 17** Top 20 highly ranked color triplets and the corresponding images they come from.

(PCA) over five-fold cross validation. The results shown utilize the best regularization parameter in each experiment. Since the PCA resulted in a significant reduction in accuracy, we chose to performed all the experiments with the entire feature set.

Knowing the features are fairly discriminative a regression analysis was performed. The regression model is likely to be unbiased when the data is uniformly distributed across ratings on the contrary a skewed distri-

**Table 2** Classification accuracy of images with high aesthetic ratings and low aesthetic ratings obtained by various thresholds

Thresholds	No. of images	Without PCA	With PCA
$4 \geq \& \leq 6.5$	452	0.812	0.768
$4 \geq \& \leq 6$	1143	0.891	0.889
$5 \geq \& \leq 6$	2638	0.703	0.702



**Fig. 18** The most aesthetically pleasing color triplets and their confidence scores from images of different ratings: (a) to (f) have ratings between 89.71 and 97.29 (high), (g) to (l) between 70.00 and 84.86 (middle), and (m) to (r) between 20.00 and 55.14 (low). The ratings are scaled from (0, 7)(ratings from *photo.net*) to (0, 100).



**Fig. 19** Exemplar images with aesthetic ratings and confidence levels predicted by our system.

bution might bias it assign mean scores very frequently. We divided the dataset into separate test and training set, the training set was created by uniformly sampling 1800 images across the ratings and the rest was used as a test set. A regression model using independent polynomials  $f$ ,  $f^{\frac{1}{3}}$ ,  $f^{\frac{2}{3}}$ ,  $f^2$  was constructed, each polynomial represents the features. Linear regression was preferred to Support Vector Regression in order to avoid over fitting. The Mean of Squared Error (MSE) for the predicted ratings was found to be 0.5916. The co-efficient of determination  $R^2$  determined by Equation 4 where  $\hat{y}$  is the predicted value from the regression and  $\bar{y}$ , the average score of the training images was found to be 0.4272.  $R^2$  determines the amount of variability in the data which the model is able to predict, representing the goodness of fit. In order to provide ratings which are consistent with our previous system ACQUINE, the model was later retrained with the average ratings scaled between 1 – 100. Some of the images with aesthetic quality ratings along with their confidence intervals with 95% confidence level are shown in Figure 19. The confidence interval of the predicted value is given by  $\hat{y} \pm t^* s_{\hat{y}}$ , where  $t^*$  is the upper 0.025 p-value for the t-distribution of the dataset. We have used the linear regression toolbox in R to generate the confidence in-

terval. We can infer that a wider confidence interval implies higher uncertainty in the aesthetic quality of the image.

$$R^2 = 1 - \frac{\sum_i (y_i - \hat{y})^2}{\sum_i (y_i - \bar{y})^2} \quad (4)$$

Any literature so far has dealt with generic models of image aesthetics alone. Due to the absence of previous works on gray scale image aesthetics or any standard dataset which can be used for evaluation and comparison we have evaluated our model over a separate test set extracted from `dpchallenge.com`. The test set consisted of about 4500 images. The Scatter plot in Figure 20 shows the predicted ratings provided by our gray scale model with the actual ratings obtained from the website. The mean squared error for the test set was found to be 0.5583.

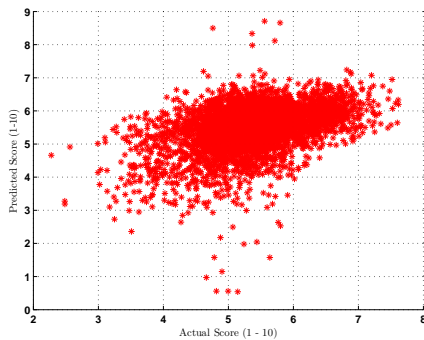


**Fig. 20** Scatter plot of predicted ratings by our model and the actual ratings.

## 5.2 Composition Feedback Examples

The above modules are integrated into the OSCAR system to provide users with feedback on each aesthetics component. Feedback is provided in the form of retrieved photographs, most aesthetically pleasing color triples and their confidence values (only for color images), and aesthetic scores for both color and gray-scale images. Similar photographs can be retrieved from the server based on visual similarity, composition categorization and aesthetic scores. The system is able to assist users with automatic composition analysis and color evaluation. The aesthetic ratings give an assessment of the photo quality in terms of general features.

We use the SIMPLIcity system to obtain the original ranking of images according to their visual similarity with the query image, and return  $K = 100$  top

ranked pictures. When users choose to re-rank the images by composition or rating, the system re-ranks these  $K$  images using the schema provided in section 2.5. Figure 21 presents 6 query examples including 4 color images and 2 gray-scale image. The photographs retrieved from the database are re-ranked by composition categories and aesthetic scores. The feedback also includes the best color triplets and their confidence scores, the composition categorization result, and machine generated aesthetic scores. ACQUINE system provides aesthetic scores for color images and the black and white aesthetics model introduced in this paper estimates aesthetic scores for gray scale images. Composition sensitive retrieval results and the original image ranking by SIMPLIcity for the same set of images are provided in Figure 22. We can see that introducing composition categorization lowers the ranks of compositionally irrelevant images, and returns more interesting pictures.

## 6 User Study and Evaluation

In this section, we investigate the usefulness of OSCAR for the users to take better photographs. Professional photographers would be ideal subjects for our user studies. However, due to time constraints, we could not invite sufficient number of professionals to participate. We finally recruited around 30 students, most of whom are graduate students at Penn State with a fair knowledge of digital images and photography. We expect to collect more feedbacks from skilled photographers in the future to improve the system. The entire demo system will be made available for public use when this work has been published. In total, three user studies have been conducted. All the photos used in these studies are from `photo.net`, the same collection used in our experiments. The detailed design and the evaluation of each user study are reported in the following sections.

### 6.1 User Perception on Composition Layout

A collection of around 1000 images were randomly picked to form the dataset for the study on composition. Each participant is provided with a set of 160 randomly chosen images and is asked to describe the composition layout of each image. At an online site, the participants can view pages of test images, beside each of which are selection buttons for seven composition categories: “Horizontal”, “Vertical”, “Centered”, “Diagonal (upper left, bottom right)”, “Diagonal (upper right, bottom left)”, “Patterned”, and “None of Above”. Multiple choices are allowed. We used “Patterned” for the class of photos with homogeneous texture (the so called “Textured”



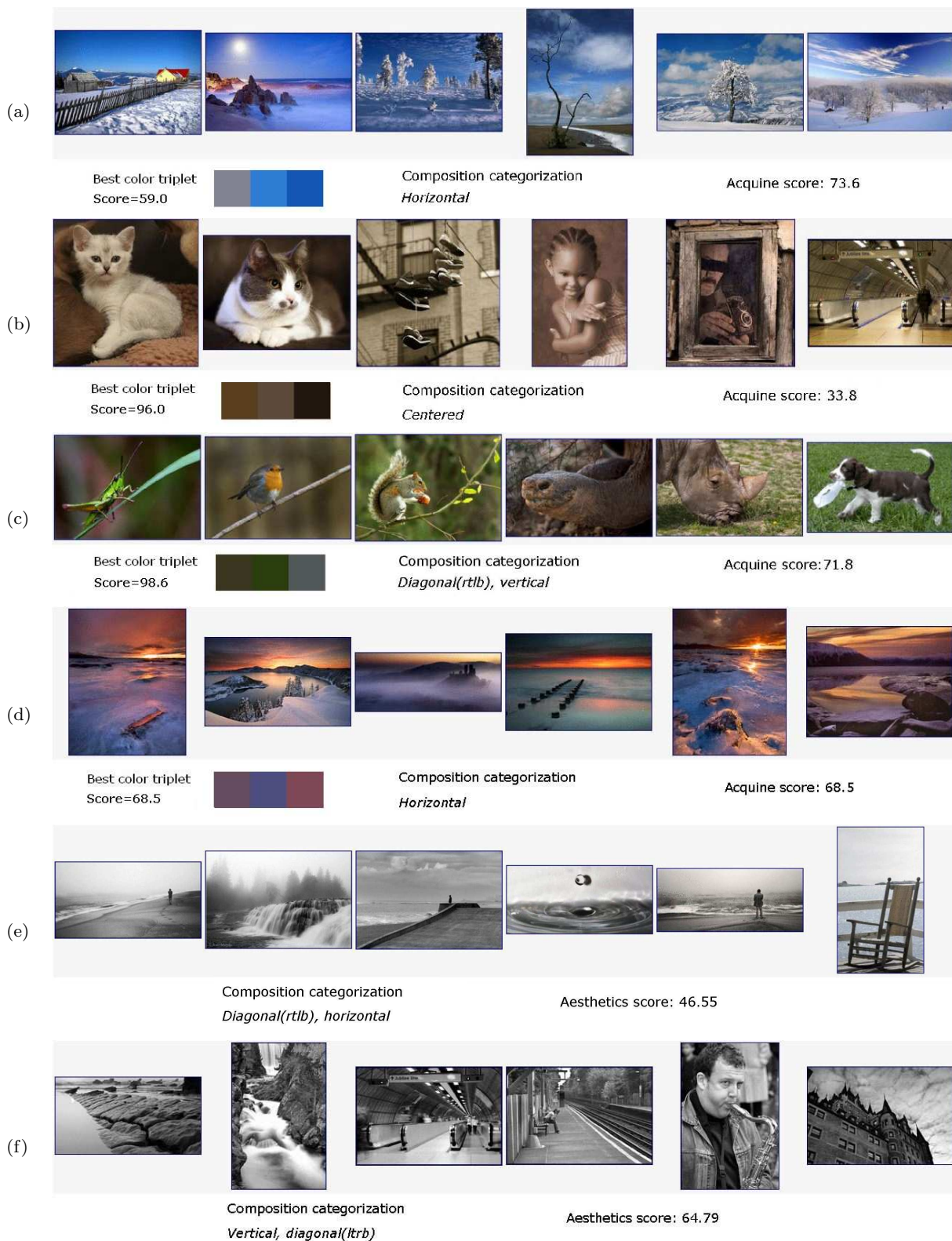


**Fig. 21** Composition feedback. Above: photographs re-ranked by composition categorization and aesthetic score. Below: the most aesthetically pleasing color triplet(only for color images) and its confidence score, composition categorization result and aesthetic score.

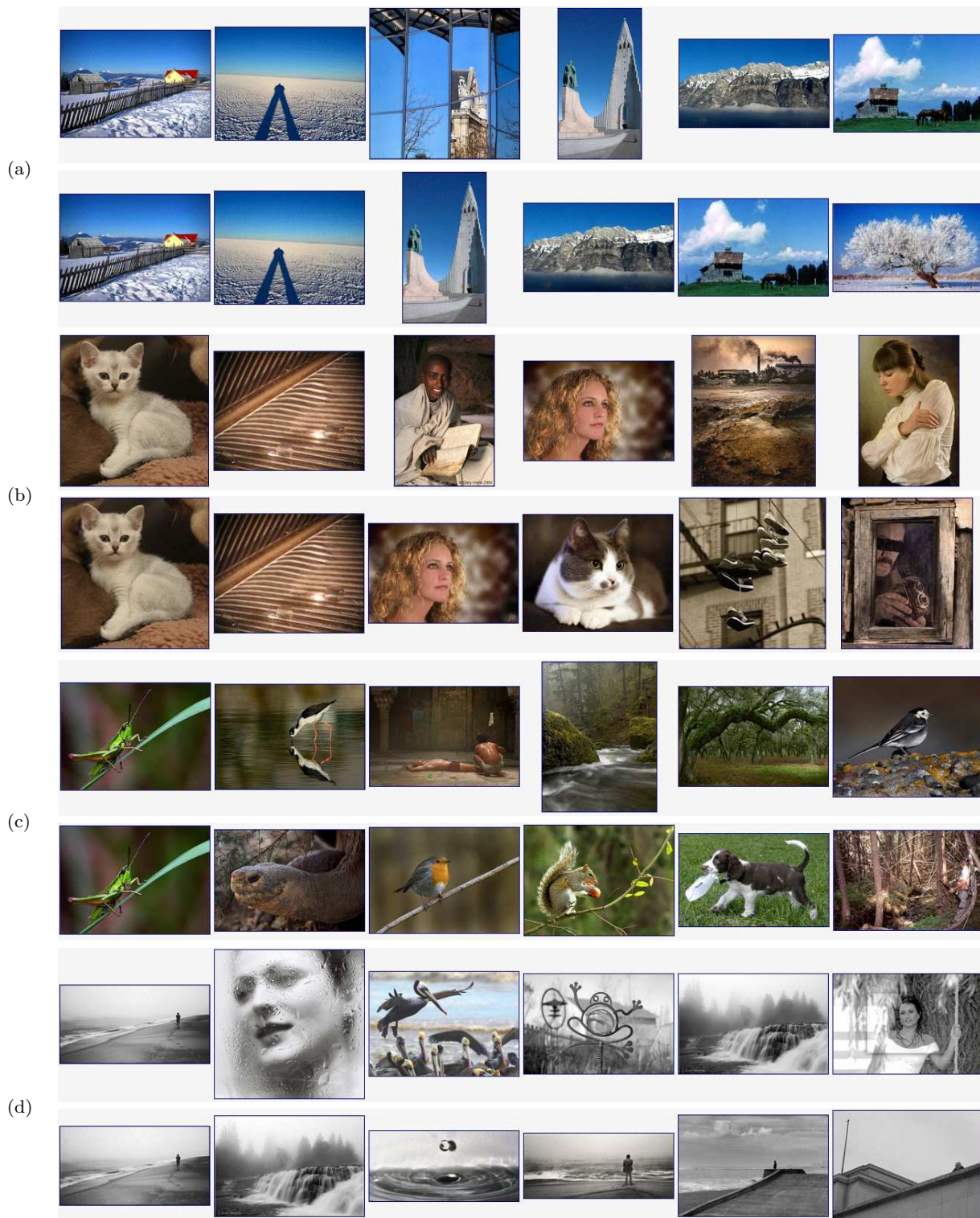


**Fig. 22** Photographs retrieved from the database. Above: ranking by visual similarity. Below: re-ranking by composition categorization.

**Table 3** Distribution of the entropy for the votes of users. For each composition category, the percentage of photos yielding a value of entropy in any bin is shown.

	[0,0.5]	(0.5,1.0]	(1.0,1.5]	(1.5,2.0]	(2.0, 2.5]
h	36.12	29.96	17.18	15.42	1.32
v	12.98	45.67	19.71	20.19	1.44
c	25.36	45.48	13.12	14.87	1.17
ulbr	12.99	44.16	19.48	19.48	3.90
urbl	16.87	43.37	18.07	20.48	1.20
t	10.77	36.92	10.77	36.92	4.62
none	6.59	39.56	17.58	34.07	2.20

class). We added the “None of Above” category to allow more flexibility for the user perception. At the end, we were able to collect 924 images that were voted by three or more users.

### 6.1.1 Variation in Users’ Choices of Composition

In order to understand compositional clarity, we examine the variation in users’ votes on composition layout. We quantify the ambiguity in the choices of composition layout using entropy. The larger the entropy in the votes, the higher is the ambiguity in the compositional layout of the image. The entropy is calculated by the formula  $\sum p_i \log 1/p_i$ , where  $p_i, i = 0, \dots, 6$ , is the percentage of votes for each category. The entropy was calculated for all 924 photos and its value was found to range between 0 and 2.5. We divided the range of entropy into five bins. The photos are divided into seven groups according to the composition category receiving the most votes. In each category, we compute the proportion of photos yielding a value of entropy belonging to any of the five bins. These proportions are reported in Table 3. We observe that among the seven categories, “Horizontal” and “Centered” have the strongest consensus among users, while “None of above” is the most ambiguous category.

### 6.1.2 Composition Classification Results

We evaluate our composition classification method in the case of both exclusive classification and non-exclusive classification. The users’ votes on composition are used to form ground truth, with specifics to be explained shortly. We consider only six categories, i.e. “Horizontal”, “Vertical”, “Centered”, “Diagonal\_ulbr”, “Diagonal\_urbl” and “Textured” for this analysis. The “None of above” category was excluded for the following reasons.

- The “None of above” category is of great ambiguity among users, as shown by the above analysis.

**Table 4** Confusion table for exclusive classification of 494 images into six composition categories. Each row corresponds to a ground truth class.

	h	v	c	ulbr	urbl	t
h	107	0	20	3	8	4
v	1	32	39	3	2	10
c	10	7	132	8	11	12
ulbr	4	0	5	18	0	2
urbl	2	1	13	0	22	1
t	0	2	6	0	0	9

- Only a very small portion of images are predominantly labeled as “None of above”. Among the 924 photos, 17 have three or more votes on “None of above”.
- We notice that these 17 “None of above” photos vary greatly in visual appearance; and hence it is not meaningful to treat such a category as a compositionally coherent group. It is difficult to define such a category. A portion of images in this category show noisy scenes without focused objects, which may become a new category to be considered in our future work.

We conducted exclusive classification only on photos of little ambiguity according to users’ choices of composition. The number of votes a category can receive ranges from zero to five. To be included in this analysis, a photo has to receive three or more votes for one category (that is, the ground-truth category) and no more than one vote for any other category. With this constraint, 494 images out of the 924 are selected. Table 4 is the confusion table based on this set of photos.

We see that the most confusing category pairs are “Vertical” vs “Centered” and “Diagonal\_urbl” vs “Centered”. Figure 23(a) shows some examples labeled “Vertical” by users while classified as “Centered” by our algorithm. We observe that the misclassification is mainly caused by the following: 1) “Vertical” images in the training dataset cannot sufficiently represent this category; 2) users are prone to label images with vertically elongated objects “Vertical” although such images may be “Centered” in the training data; 3) the vertical elements fail to be captured by image segmentation. Figure 23(b) gives “Diagonal\_urbl” examples mistakenly classified as “Centered”. The failure to detect diagonal elements results mainly from: 1) diagonal elements which are beyond the diagonal tolerance set by our algorithm; 2) imaginary diagonal visual paths, for example, the direction of an object’s movement.

In non-exclusive classification, the criterion for a photo being assigned to one category is less strict than in the exclusive case. A photo is labeled as a particular category if it gets two or more votes on that category.

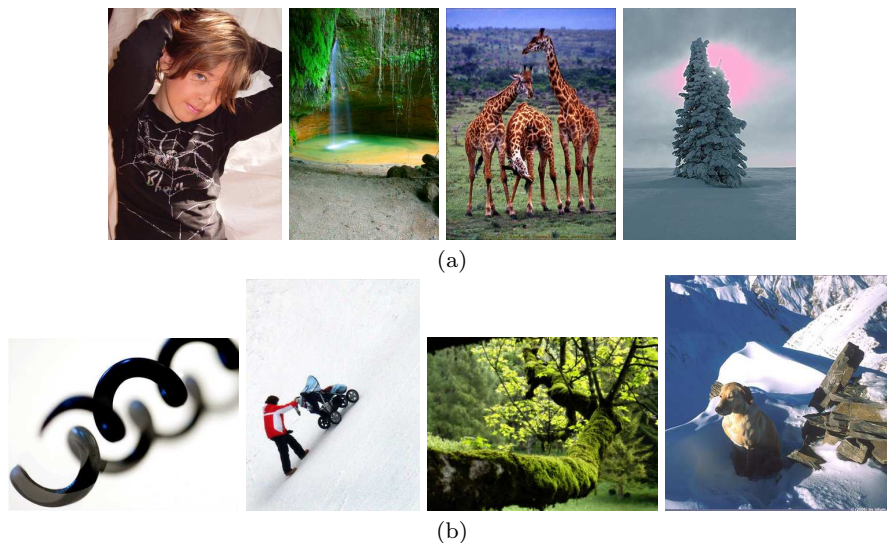


**Fig. 23** Photo examples mistakenly classified as “Centered” by our algorithm. (a) Photos labeled “Vertical” by users; (b) Photos labeled “Diagonal\_urbl” by users.

In total there are 849 out of the 924 photos with at least one category voted twice or more. The results reported below is based on these 849 photos.

The composition categorization of a photo is represented by a six-dimensional binary vector, with 1 indicating the presence of a composition type, and 0 the absence. Let  $M = (m_0, \dots, m_5)$  and  $U = (u_0, \dots, u_5)$  denote the categorization vector generated by our algorithm and by users respectively. The value  $m_0$  is set to 1 if and only if there are 10 or more nearest neighbors (among 30) labeled as “Horizontal”. The values of  $m_1$  and  $m_2$ , corresponding to the “Vertical” and “Centered” categories, are set similarly. For the diagonal categories,  $m_i$ , where  $i = 3, 4$ , is set to 1 if any diagonal element is detected by our algorithm. Finally,  $m_5$  is set to 1 if the “Textured” versus “Non-textured” classifier labels the image “Textured”. Three ratios are computed to assess the accuracy of the non-exclusive classification.

- Ratio of partial detection  $r_1$ : the percentage of photos for which at least one of the user labeled categories is declared by the algorithm. Based on the 849 photos,  $r_1 = 80.31\%$ .
- Detection ratio  $r_2$ : the percentage of photos for which all the user labeled categories are captured by the algorithm. Define  $M \succ U$  if  $m_j \geq u_j$  for any  $j \in [0, 5]$ . So  $r_2$  is the percentage of images for which  $M \succ U$ . We have  $r_2 = 66.00\%$ .
- Ratio of perfect match  $r_3$ : the percentage of photos for which  $M = U$ . We have  $r_3 = 33.11\%$ .

The precision of the algorithm can also be measured by the number of mismatches between  $M$  and  $U$ . We

say a mismatch occurs if  $m_j \neq u_j$ ,  $j = 0, \dots, 5$ . We count the number of mismatches for every image and plot the histogram of these counts in Figure 24.

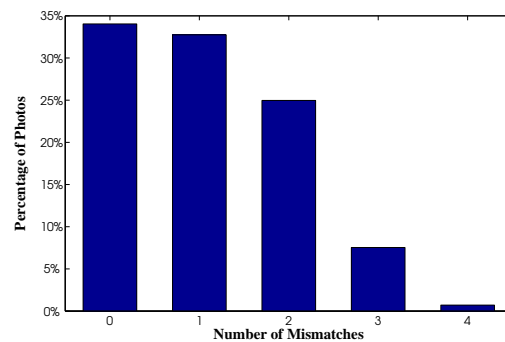


**Fig. 24** Histogram of the number of mismatches between classification by our algorithm and by the users. The horizontal axis corresponds to the number of mismatches. The vertical axis corresponds to the percentage of photos.

## 6.2 Evaluation of Retrieved Exemplars

Every user study participant was provided with 15 randomly chosen query images. For each query, we show the participant the combined set of photos retrieved in the top eight images by each of the three ranking schemes based respectively on visual similarity, composition relevance, and aesthetic appeal. We removed the duplicates and shuffled the photos to avoid any redundancy and biases. For each photo, the participants were asked the following “yes/no” questions:

1. Is this photo semantically similar to the query image?
2. Is this photo compositionally relevant to the query image?
3. Is this photo aesthetically appealing?

For each ranking scheme, the percentages of retrieved photos that users indicated as semantically similar/ compositionally relevant/ aesthetically appealing were calculated. Figure 25 compares the performance of the three different ranking schemes. For the top four retrieved images, the re-ranking scheme based on composition yields the best result on all the three accounts; and the re-ranking based on both composition and aesthetics yields the second best. The margin of improvement over the baseline scheme (no re-ranking) is substantial. For the top eight retrieved images, the two re-ranking schemes are still consistently better than without re-ranking. In terms of semantic similarity and compositional relevance, the re-ranking by composition alone is better than re-ranking by both composition and aesthetics; while in terms of aesthetic appeal, the latter is slightly better. The fact that re-ranking by composition improves semantic similarity reflects a positive association between composition and semantics. Images that are composed similarly tend to agree more semantically.

### 6.3 User Perception on Feedbacks

Each user study participant is shown with Web pages displaying the feedbacks OSCAR provides for ten randomly assigned photos. For each photo, the feedbacks include:

- Best color triplet: the most aesthetically appealing color combination found in the query photo.
- Confidence score of the color triplet: a floating number from 0-100, indicating a triplet’s aesthetic quality (100 indicates the best quality), shown beside the triplet.
- Aesthetic score: a score profiling the aesthetic quality of the query photo in general, shown as stars (five stars indicate the best quality).
- Photo exemplars: high quality photographs used for reference in terms of composition, coloring, etc. We use the re-ranking scheme based on both composition and aesthetics.

Participants are asked to assume that they are the photographers who have taken these photos and to evaluate whether the feedbacks can help improve their photography skills, in terms of composition, coloring, in a general sense. Each participant is requested to indicate her/his level of agreement with the following five statements.

1. The color combination score reflects your impression about the color triplet.
2. The aesthetic score is consistent with your assessment of the photo’s aesthetic quality.
3. Some of the photo exemplars can potentially help improve your photography composition.
4. The color triplets can potentially help improve your coloring scheme.
5. The overall feedback can potentially help improve your photography skills in general.

The response preference for each statement is based on a 5-point likert scale, i.e., “strongly agree”, “agree”, “neither agree nor disagree”, “disagree” and “strongly disagree”. A screen shot of the user study interface is shown in Figure 26.

For each statement, we calculated the percentage of votes for every agreement level. For a clearer graphical presentation, we combine the two positive levels “strongly agree” and “agree”, and similarly the two negative levels “disagree” and “strongly disagree”. Figure 27 shows the distribution of votes on “agree”, “neither agree nor disagree”, and “disagree” for the five statements listed above. In the figure, every group of bars is the result for one statement, arranged from left to right in the same order as in the list above. A majority of votes support the value of the individual modules in the feedback as well as the usefulness of the overall system. For the individual modules, users are most positive about the exemplar photos.

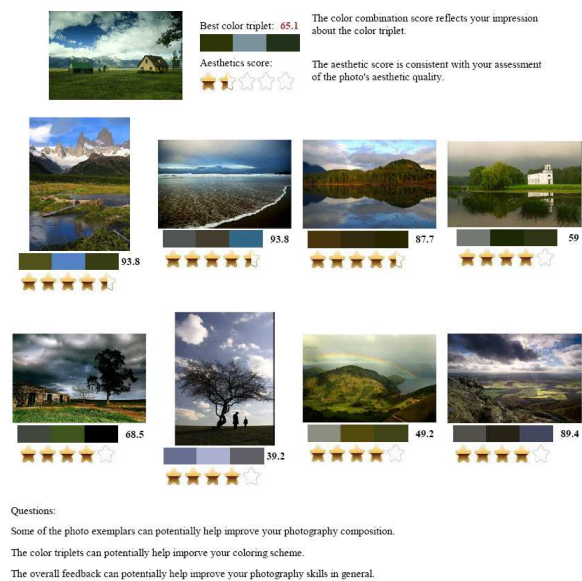


**Fig. 26** A screen shot of the web interface for analyzing user perceptions on feedbacks.

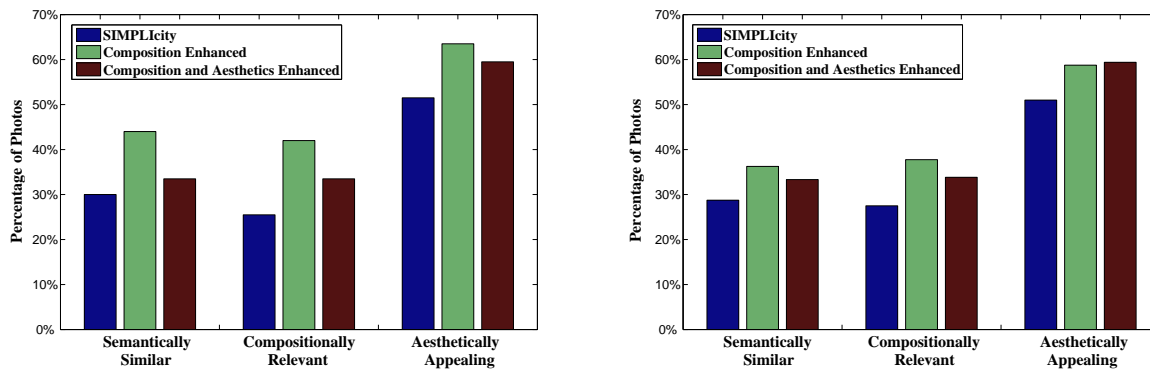


**Fig. 25** Retrieval accuracy in terms of “semantically similar”, “compositionally relevant” and “aesthetically appealing” for different ranking schemes. Left: results based on top 4 retrieved images. Right: results based on top 8 retrieved images.

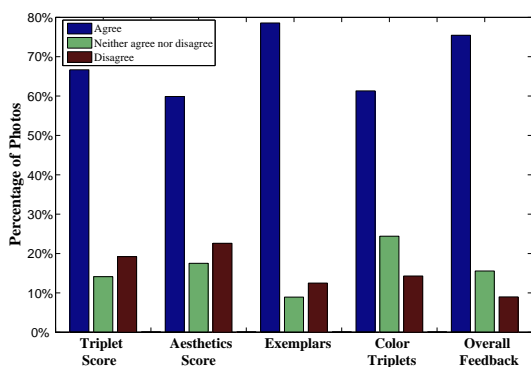


**Fig. 27** Distribution of user votes in response to the five statements we made on module feedback and overall feedback.

## 7 Running Time

We hereby report the running time of OSCAR. The modules of OSCAR are tested on a single compute node with 2 quadcore Intel processors running at 2.66 GHz and 24 GB of RAM. For the composition analysis module, the average time to process a  $256 \times 256$  image is 3.15 seconds, including image segmentation (Li 2011), edge detection (Meer and Georgescu 2001), and composition classification proposed in this paper. For the color combination feedback module, the average time of segmenting an image and obtaining its color triplets with hierarchical mode association clustering (HMAC) algorithm (Li et al. 2007) is 0.58 second while computing the confidence score of the best color triplet takes 0.53 second. Computing aesthetic scores for gray-scale images takes an average of 1.89 seconds including image segmentation, feature extraction and score generation. Initializing retrieval results by SIMPLicity incurs very low overhead which can be further reduced when running in parallel with other modules. Therefore, for a given image, all the feedback can be provided within a few seconds.

## 8 Conclusions and Future Work

We have presented a next generation aesthetic assessment system which is able to provide substantially reliable feedback to the users on improving the aesthetic quality of their photographs as well as providing an assessment on the quality of the images. We bring together various characteristics of a highly aesthetic photograph in order to provide comprehensive feedback on the feature chosen by the user.

Motivated by an old adage, “*I hear, I know. I see, I remember. I do, I understand.*” we believe that practicing is the best way of learning. We try to provide feedback which lets the user learn and infer aesthetic composition characteristics through high quality exemplars. In order to accomplish this we have been able to successfully classify five categories of spatial image composition with reliable accuracy leading us to retrieve images of similar composition with a good precision.

We also assist the user in choosing better color combination by providing a quantitative feedback on the presence of aesthetically pleasing color triplets in the photograph. These color triplets are learnt through a data driven approach, with quantitative values indicating the confidence about their aesthetics.

Last but not the least we have also demonstrated the usefulness of a newer module to assign aesthetic ratings to monochromatic images by evaluating the discriminative power of the visual features. The regression model learnt is able to predict 75.33% of the variability in the noisy ratings. This provides a completion to our pre-existing ACQUINE system which can predict reliable aesthetic ratings of color images. This form of a feedback can be considered both quantitative as well as collective in nature.

## 8.1 Future Work

Our composition and aesthetics feedback system is a prototype. Because of the inherent complexity of aesthetics and the multifaceted nature of picture composition, there is ample room for extension and enhancement in the future.

The five categories of composition can be refined further to include more classes. Our current usage of the spatial signature of an image is quite restrictive, only to classify the composition. We can employ the spatial signature more quantitatively so that the difference in composition is not just categorical agreement or disagreement. For instance, a new pairwise distance between images can be defined to incorporate the spatial signature with the conventional color and texture signature.

A significant step beyond the present analysis of composition is to make on-site automatic suggestions about placement of objects in a photo, which can be achieved by zooming, expanding, tilting, etc. Principles of good composition can be applied based on composition characteristics extracted by the computer. For instance, the diagonal spatial structure provides a sense of dynamism in the image and is highly pleasing. Adjustment made to the image frame to diagonalize the not-so diagonal element can increase the image aesthetics.

New functions can be added in color feedback module to make suggestions about the color temperature, white balance and lighting of the subject, etc. Our color feedback framework can be tested on more color models in order to find the best one for real applications.

The aesthetic feedback system can be improvised by the addition of complex features which can reflect upon the symmetry and forms of the objects present in the image.

Finally, the system improvement lies in making it distributive which can increase the speed of computation by allocating modules to different servers.

**Acknowledgements** We thank the reviewers and editors for their comments and suggestions. Undergraduate students Razvan Orendovici, John Schleicher, and David Zhang assisted in the prototype development. This material is based upon work supported by the National Science Foundation under Grant Nos. 0347148 and 0936948. The computational infrastructure was provided by the Foundation through Grant No. 0821527. Part of the work of J. Z. Wang is done while working at the Foundation. Any opinion, findings, and conclusions or recommendations expressed in this material are those of the authors and do not necessarily reflect the views of the National Science Foundation.

## References

- Bhattacharya, S., Sukthankar, R., and Shah, M. (2010). A coherent framework for photo-quality assessment and enhancement based on visual aesthetics. In *Proceedings of ACM Multimedia conference* (pp. 271-280).
- Cohen-Or, D., Sorkine, O., Gal, R., Leyvand, T. and Xu, Y. (2006). Color harmonization. *ACM Transactions on Graphics*, 25(3), 624-630.
- Datta, R., Joshi, D., Li, J. and Wang, J. Z. (2006). Studying aesthetics in photographic images using a computational approach. In *Proceedings of European conference on computer vision*, (pp. 288-301).
- Datta, R. and Wang, J. Z. (2010). ACQUINE: aesthetic quality inference engine - real-time automatic rating of photo aesthetics. In *Proceedings of international conference on multimedia information retrieval*, (pp. 421-424).
- Davis, H. (2010). Creative black and white. *Digital Photography Tips and Techniques*. Wiley Publishing Inc.
- Feininger, A. (1973). *Principles of composition in photography*. Thames and Hudson Ltd.
- Folts, J. A., Lovell, R. P., and Zwahlen, F. C. (2005). *Handbook of photography*. Thompson Delmar Learning.
- Fogarty, J., Forlizzi, J. and Hudson, S. E. (2001). Aesthetic information collages: generating decorative displays that contain information. In *Proceedings of ACM symposium on user interface software and technology*, (pp. 141-150).
- Gao, X., Xin, J., Sato, T., Hansuebsai, A., Scalzo, M., Kajiwara, K., Guan, S., Valldeperas, J., Lis, M., and Billger, M. (2007). Analysis of cross-cultural color emotion. *Color Research and Application*, 32(3), 223-229.
- Gersho, A., Asymptotically optimal block quantization. (1979) *IEEE Transactions on Information Theory*, 25(4), 373-380.
- Gill, M. (2000). *Color harmony pastels - a guidebook for creating great color combinations*. Rockport Publisher.
- Harel, J., Koch, C., and Perona, P. (2007). Graph-based visual saliency. In *Proceedings of advances in neural information processing systems*, (pp. 542-552).
- Henri, R. (2007). *The Art Spirit*. Basic Books.
- Itten, J. (1960). *The Art of Color*. New York: Van Nostrand Reinhold.
- Karatzoglou, A., Smola, A., Hornik, K., and Zeileis, A. (2004) kernlab - a package for kernel methods in R. *Journal of Statistical Software*, 11(9), 1-20.
- Ke, Y., Tang, X. and Jing, F. (2006). The design of high-level features for photo quality assessment. In

- Proceedings of IEEE conference on computer vision and pattern recognition*, (pp. 419-426).
- Kisilev, P., Shaked, D., and Lim, S. (2007). Noise and signal activity maps for better imaging algorithms. In *Proceedings of IEEE international conference on image processing*, (Vol. 2, pp. 117-120).
- Krages, B. P. (2005). *Photography: the art of composition*. Allworth Press.
- Lamb, J., and Stevens, R. (2010). Eye of the Photographer. *The Social Studies Texan*, 26(1), 59-63.
- Levina, E., Bickel, P. (2001). The Earth Mover's Distance is the Mallows Distance: Some Insights from Statistics. In *Proceedings of international conference on computer vision*, (pp. 251-256).
- Li, J. (2011). Agglomerative Connectivity Constrained Clustering for Image Segmentation. *Statistical Analysis and Data Mining*, 4(1), pp. 84-99.
- Li, J., Ray, S. and Lindsay, B. G. (2007). A nonparametric statistical approach to clustering via mode identification. *Journal of Machine Learning Research*, 8(8), 1687-1723.
- Li, J., Wang, J. Z., and Wiederhold, G. (2000). IRM: integrated region matching for image retrieval. In *Proceedings of ACM multimedia conference*, (pp. 147-156).
- Liu, L., Chen, R., Wolf L. and Cohen-Or, D. (2010). Optimizing photo composition. *Computer Graphic Forum*, 29(2), 469-478.
- Luo, Y. and Tang, X. (2008). Photo and video quality evaluation: focusing on the subject. In *Proceedings of European conference on computer vision*, (pp. 386-399).
- Mallows, C. L. (1972) A note on asymptotic joint normality. *Annals of Mathematical Statistics*, 43(2), 508-515.
- Manav, B. (2007). Color-emotion associations and color preferences: a case study for residences. *Color Research and Application*, 32(3), 144-150.
- Meer, P. and Georgescu, B. (2001). Edge detection with embedded confidence. *IEEE Transactions on Pattern Analysis and Machine Intelligence*, 23(12), 1351-1365.
- Obrador, P., Anguera, X., Oliveira, R. and Oliver, N. (2009). The role of tags and image aesthetics in social image search. In *Proc. ACM SIGMM workshop on social media*, (pp. 65-72).
- Obrador, P., Oliveira, R. and Oliver, N. (2010). Supporting personal photo storytelling for social albums. In *Proceedings of ACM multimedia conference*, (pp. 561-570).
- Peters, G. (2007). Aesthetic Primitives of Images for Visualization. In *Proceedings of IEEE International Conference on Information Visualization*, (pp. 316-326)
- Rubner, Y., Tomasi, C., and Guibas, L. J. (2000). The earth mover's distance as a metric for image retrieval. *International Journal of Computer Vision* 40(2), 99-121, 2000
- Russ, J. C. (2006). *The image processing handbook*. CRC Press.
- Speed, H. (1972). *The practice and science of drawing*. 3rd Ed. Dover Publications.
- Sternberg, R. J. (2008). *Cognitive psychology*. Wadsworth Publishing.
- Suess, B. J. (1995). *Mastering black and white photography: from camera to darkroom*. Allworth Press.
- Sutton, T., Whelan, B. M. (2004). *The complete color harmony*. Rockport Publisher.
- Taylor, M., Butler, O. and Birnbaum, H. (1998). *Kodak workshop series: advanced black-and-white photograph*. Sterling Pub Co Inc.
- Tokumaru, M., Muranaka, N. and Imanishi, S. (2002). Color design support system considering color harmony. In *Proceedings of IEEE international conference on fuzzy systems*, (Vol. 1, pp. 378-383).
- Tong, H., Li, M., Zhang, H. and Zhang, C. (2004). Blur detection for digital images using wavelet transform. In *Proceedings of IEEE international conference on multimedia & expo*, (pp. 17-20).
- Wang, J. Z., Li, J., and Wiederhold, G. (2001). SIMPLiCity: semantics-sensitive integrated matching for picture libraries. *IEEE Transactions on Pattern Analysis and Machine Intelligence*, 23(9), 947-963.
- Wong, L. and Low, K. (2009). Saliency-enhanced image aesthetics class prediction. In *Proceedings of IEEE international conference on image processing*, (pp. 993-996).
- Warren, B. (2002). *Photography: the concise guide*. Delmar Cengage Learning.